



POLITECNICO
DI TORINO



TU Delft



EXPERIMENTAL STUDY OF EXTERNAL AS WELL AS INTERNAL CORE FORMATION DAMAGE

HESHAM BASAL

Experimental Study of External as well as Internal Core Formation Damage

By

Hesham Basal

Supervisors:

Prof. Dr. Pacelli Zitha (Delft University of Technology)

Prof. Dario Viberti (Politecnico di Torino)

Thesis is submitted in compliance with the requirements for
the Master of Science degree of Petroleum Engineering
at Politecnico Di Torino
(December 2019)

Abstract

Water injection is always considered the optimum technique for recovery of additional oil from mature fields, as it can be used to support the reservoir energy as a secondary recovery method. It can also be part of the waste water management industry, where the produced water is filtered and re-injected to the ground. Apart from the purpose of water injection, the phenomenon of low injection is always linked to water injection projects. One of the main reasons for this phenomenon is the solid particles that are suspended in water. These solid particles are filtered by the porous medium and are retained in the pores of the grains matrix.

Water quality is considered one of the most important factors that affect the injectivity decline phenomenon. In the first part of this study, water quality has been characterized by studying the stability of the suspended solid particles in water in order to determine the optimum conditions of salinity, PH and suspended solid particles size and concentration at which the effect of flocculation and coagulation is very low. By the end of this study a certain range of brine salinity, PH and suspended solid particles size and concentration were selected to be used in the second part of this research.

After that, Core flooding experiments were conducted on Bentheimer sandstone core plugs using brine solution representing the North Sea composition and Baracarp solid particles (CaCO_3) at different flow rate. Pressure measurements were obtained along the core in order to analyse the retention of the suspension particles along the core plug. Moreover, the influent and effluent samples were taken during the core flood experiments to study the change in the suspension concentration and how the core plug is acting as a filter.

It was obvious from the characterization phase that the hydrodynamic particle size in different brine samples is always larger than the actual particle size. As the brine salinity increase, the average particle size increase. There is a specific PH range at which the lower value of the hydrodynamic average particle size in the brine was observed. The concentration of particles in brine has no clear effect on the hydrodynamic average particle size. The pressure drop profile did not show a linear relation with the total pore volume injected. The internal core damage was limited and had a lower effect on the total pressure drop. However, the external core damage (External filter cake) had a higher effect on the pressure drop.

Acknowledgement

First of all I would like to dedicate this work to my wife, mom and dad for their love and continuous support through the all stages of my life. To my little daughter, you always give me hope and motivation to keep going.

I would like to thank Prof. Pacelli Zitha for his invitation to work on this research and his guidance and supervision from the first day. I would like to present my thanks to Prof. Dario Viberti for his support and help during the project. Moreover, this research would not be done without the help of my lab supervisor Dr. Sian Jones. Thanks Sian for all you have done to teach and help me. I would like also to thank Michiel Slob for his help in preparing the experiment set up.

Finally, many thanks and appreciation to the subsurface team at Shell, to Katie Humphry, Marco Welling, Frank van der Heyden, Shikha Rath and Ron Bouwmeester for their incredible support and encouragements, their expertise and professionalism.

Contents

Chapter One: Introduction.....	12
1.1 Waterflooding	13
1.2 Objectives of the Research	15
1.3 Approach.....	15
1.4 Thesis Outlines	15
Chapter Two: Theory	17
1.1. Formation Damage.....	17
1.2. Deposition Profile and Retention Sites.....	18
1.3. Retention Mechanisms	20
2. Water Quality	24
2.1. Solid particles	24
2.2. Influence of Salt Concentration	24
2.3. Influence of pH.....	25
2.4. DLVO Theory	25
2.5. Electric Double Layer	25
2.6. Zeta Potential (ζ).....	26
2.7. Electrophoretic Mobility.....	26
3. Forces Acting On a Particle In a Colloidal System.....	27
3.1. Drag Force.....	27
3.2. Lift Force	28
3.3. Net Gravity Force.....	28
3.4. Interparticle forces	28
3.5. Diffusion	29
3.6. Friction Force	29
Chapter Three: Brine Characterization	31
3.1 Selection of Suspended Solid Particle	31
3.2 The Effect of Brine Salinity:.....	33
3.3 The Effect of PH:.....	36
3.4 The Effect of Particles Concentration:.....	38
Chapter Four: Experiments	43
4.1 Characterization of the Porous Medium:.....	43
4.2 Core Plug Preparation:	43

4.3 Experimental Set up:.....	44
4.3.1 Injection Pump	44
4.3.2 Core Holder	45
4.4 Experimental Procedure:	46
Chapter Five: Results and Discussion.....	49
5.1 Permeability Measurements:	49
5.2 Initial Brine Flow.....	50
5.3 Suspension Solution Injection.....	50
5.4 Pressure drop profile	50
5.5 Experiment CF-02.....	52
Chapter Six: Conclusion and Recommendation	55
Appendix A: Permeability Measurements	58
A.1: CF-01 (tap water)	58
A.2: CF-01 (Brine)	58
A.3: CF-01 (after the injection of 75 PV of Brine).....	59
Appendix B: Picture of the Experimental Setup	60

Table of Figures

Figure 1: Global water demand by sector to 2040.....	12
Figure 2: Water withdrawals in the energy sector, 2014.....	14
Figure 3: Particle and pore throat size distributions responsible for internal and external filtrations. (a) Pure internal filtration; Internal followed by external filtration (b) Simultaneous internal and external filtrations; (c) Pure external filtration.....	18
Figure 4: (a) Particle deposition on the rock surface; (b) Particle deposition in a constriction.	18
Figure 5: Porous medium depicting the formation of external filter cake on the injection face.	19
Figure 6: Porous medium depicting simultaneous occurrence of various mechanisms for deposition of particles.....	19
Figure 7: Retention sites in porous media a) Surface sites, b) Constriction sites, c) Crevice sites and d) Cavern sites	19
Figure 8: Illustration of particle retention mechanisms in porous medium	21
Figure 9: Surface deposition of particles in porous medium	21
Figure 10: Illustration of bridging, multi –particle and mono-particle plugging in porous media.....	22
Figure 11: External and Internal filter cake	22
Figure 12: Impact of different capture processes on varying particle size.	23
Figure 13: Schematic of the forces acting on a particle in the cake surface in a crossflow filtration process	27
Figure 14: BARACARP particle size range according to HALLIBURTON product data sheet.	32
Figure 15: (a) Pore bodies and throats diameter frequency distribution; (b) Pore bodies and throats cumulative diameter distribution.	32
Figure 16: Schematic view of the light scattering technique used by Bluewave Microtrac Particle Size Analysis	34
Figure 17: Average Particle Size Distribution for sample SA-01.....	35
Figure 18: Average Particle Size Distribution for sample SA-02.....	35
Figure 19: Average Particle Size Distribution for sample SA-03.....	35
Figure 20: Data represent the effect of salinity on the average particle size.	36
Figure 21: Average Particle Size Distribution for sample SA-01-PH-07	37

Figure 22: Average Particle Size Distribution for sample SA-01-PH-08	37
Figure 23: Average Particle Size Distribution for sample SA-01-PH-09	37
Figure 24: Data represent the effect of PH on the average particle size	38
Figure 25: Average Particle Size Distribution for sample SA-01-PPM-50	39
Figure 26: Average Particle Size Distribution for sample SA-01-PPM-100.....	39
Figure 27: Average Particle Size Distribution for sample SA-01-PPM-250.....	39
Figure 28: Average Size Particle Distribution for sample SA-01-PPM-500.....	40
Figure 29: Average Particle Size Distribution for sample SA-01-PPM-1000.....	40
Figure 30: Data represent the effect of particle concentration on the average particle size	41
Figure 31: Schematic view of the core holder and core plug	44
Figure 32: The schematic view of the experimental setup.....	46
Figure 33: Pressure Drop Profile data along the core	51
Figure 34: Injectivity Decline along the 1st core	51
Figure 35: Pressure Drop Profile data along the 2nd core.....	53
Figure 36: Injectivity Decline along the 2nd core	53

Chapter One: Introduction

“Energy needs water, water needs energy; and these linkages have enormous significance for economic growth, life and well-being.”, this how the International Energy Agency described the strong relation between water and energy at the World Energy Outlook in 2016. Water is required for all the phases of energy production, for oil and gas extraction, transport and processing, power production and irrigation of feedstock for biofuels. Water can also be produced as a by-product of oil production. On the other hand, energy is needed for many of water-related operations, such as wastewater treatment, desalination and water transport. Energy can be also produced as a by-product from wastewater treatment. Both sides of this equation come with considerable risks. The interdependencies between energy and water are set to become more intense in the coming years, as the water needs for the energy sector rise.

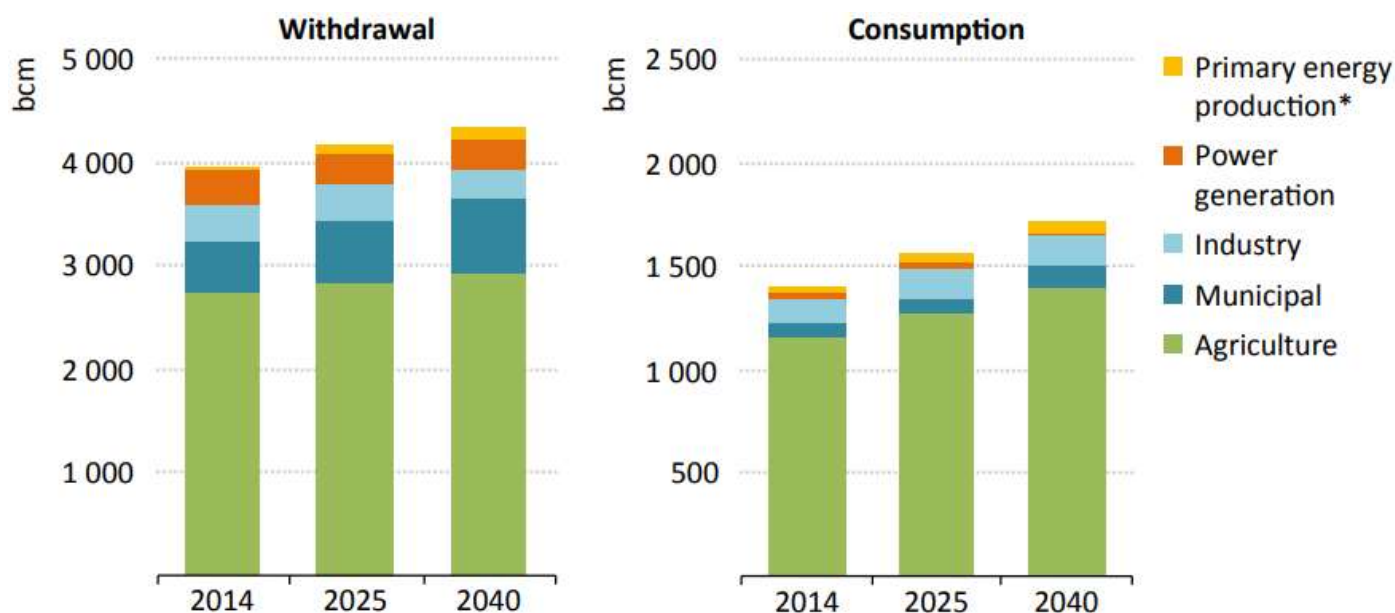


Figure 1: Global water demand by sector to 2040.

* Primary energy production includes fossil fuels and biofuels. Notes: bcm = billion cubic metres.

Agriculture is still the primary source of global water demand. However, the demand of the other sectors increases in the same time. The energy sector is responsible for 10% of global water withdrawals, mainly for power plant operation as well as for production of fossil fuels and biofuels.

1.1 Waterflooding

The stages of oil recovery process are divided into three basic stages, primary oil recovery, secondary oil recovery and enhanced oil recovery, based on the method of production or the time at which they are obtained. Primary oil recovery describes the production of hydrocarbons under the natural driving mechanisms present in the reservoir without additional help from injected fluids such as gas or water. In most cases, the natural driving mechanism is a relatively inefficient process and results in a low overall oil recovery. The lack of sufficient natural drive in most reservoirs has led to the practice of supplementing the natural reservoir energy by introducing some form of artificial drive, the most basic method being the injection of gas or water. Secondary oil recovery refers to the additional recovery that results from the conventional methods of water injection and immiscible gas injection. Usually, the selected secondary recovery process follows the primary recovery but it can also be conducted concurrently with the primary recovery. Water flooding is perhaps the most common method of secondary recovery. Enhanced oil recovery is that additional recovery over and above what could be recovered by primary and secondary recovery methods. Various methods of enhanced oil recovery (EOR) are essentially designed to recover oil, commonly described as residual oil, left in the reservoir after both primary and secondary recovery methods have been exploited to their respective economic limits.

Water injection as a means to improve oil recovery, can require large volumes of water, as much as ten-times more than primary recovery, depending on the technique. Production of extra-heavy oil, such as oil sands, is also required significant volumes of water, both for surface mining and steam-assisted gravity drainage (SAGD), where steam is used to make heavy oil flow.

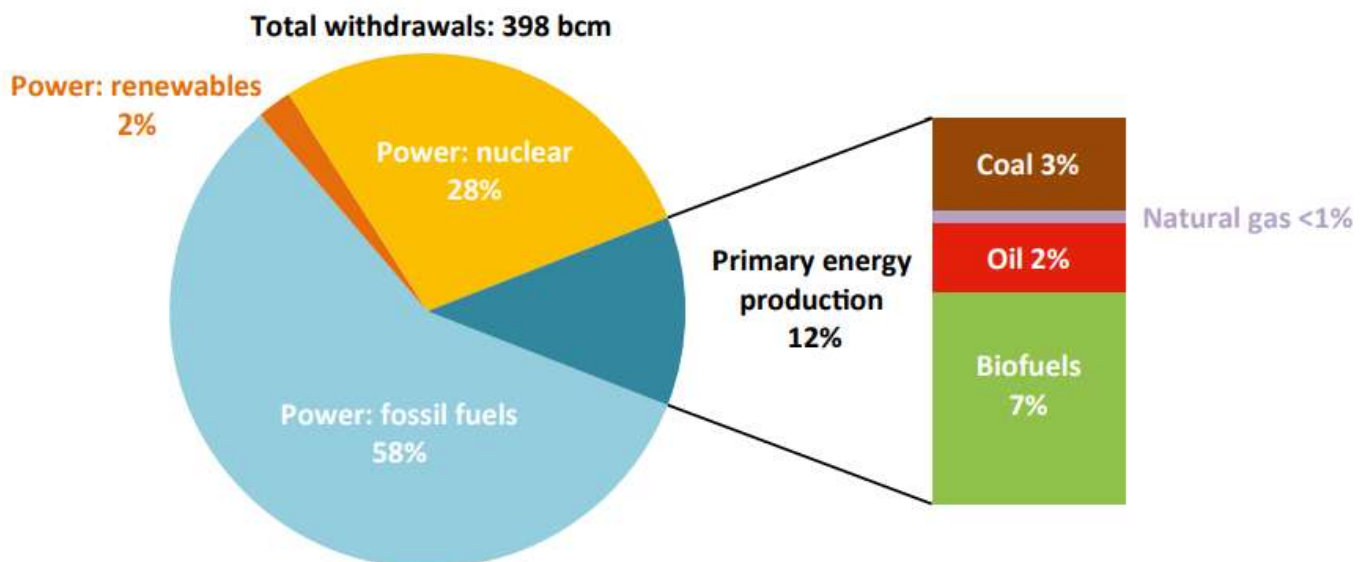


Figure 2: Water withdrawals in the energy sector, 2014.

During the injection of water into formation, there are many factors that affect the injectivity that we can summarize in three main parameters, the quality of the injected water, the reservoir heterogeneity, and the chemical reactions between the injected water and the formation matrix. The most influential factor among these previous factors is the quality of the injected water. Most of water flooding projects all over the world could not achieve their objectives due to the fact that the quality of the injected water is not compatible with the host reservoir.

The main consequence of this incompatibility is formation damage due to the injected water that causes reduction in permeability. This reduction in permeability leads to increase in the injection pressure and reduction in the injection rates. Finally, stimulation operations could become the only available option to overcome the formation damage and if the injectivity decline is not properly assessed in advance, this may lead to extensive economic losses. Several research studies have been done in this scope, but understanding the injectivity decline as a result of formation damage is still considered incomplete and there is no absolute approach.

The quality of the injected water is affected by several agents which in turn have an obvious effect on the well injectivity impairment. The presence of solid particles in water, suspension solution, is one of these agents due to the fact that as the suspension solution is injected into the porous medium, the small suspended particles tend to penetrate the formation near the wellbore and retained inside the pore throats of the formation matrix causing internal filter cake, while large suspended solid particles tend to be deposited on the injection face causing external filter cake. Both internal filter cake and external filter cake are responsible for formation damage and as a consequence injectivity decline. That is why water filtration is always required before injection in order to avoid the formation of internal and external filter cake.

Further discussion about the mechanism and the factors that contribute to the formation of internal and external filter cake will be done in chapter two.

1.2 Objectives of the Research

The main objective of this research is to answer the question of how would the water quality affect the formation damage and as a consequence the well injectivity impairment? In order to answer this question, sub research objectives have been formulated through this study. The first one is to study the stability of suspended solid particles in water under static conditions and how these conditions would be important to the water injection. The second goal is to study the effect of the quality of injected water under dynamic conditions on injectivity through the injection of different suspension solutions. The third target is to investigate the depth of penetration of the suspended solid particles in the porous medium. The final objective will be interpretation of the particles retention mechanism that happened through the injection of the suspension solution.

1.3 Approach

An experimental study was conducted based on scientific basis to achieve the objectives of this research. The first part of this study includes the preparation of brine solution that represents the sea water composition with different salinity, PH and suspended particles concentration in order to study the stability of these suspended particles in different brine conditions. Based on the results of the first part, a set of core flooding experiment was designed in the second part of this study to evaluate the decline of injectivity and the permeability reduction under different dynamic conditions.

1.4 Thesis Outlines

The research consists of six main chapters. The first one gives an introduction about the problem of injectivity decline due to water quality and the guidelines to be followed in order to achieve the objectives of this study. The second chapter covers the theories and concepts behind the work that is already done in this field. All the studies that have been done in the characterization phase to study the stability of suspended particles in different brine solutions have been mentioned in the third chapter. The fourth chapter is dedicated for the experimental setup and core flooding experiments. All the results of the core flooding experiments are summarized and discussed in details in the fifth chapter. The sixth chapter includes the conclusion of all the work done in this study.

Chapter Two: Theory

This chapter covers the theories and the concepts behind the work that is already done in the field formation damaged and well injectivity impairment. It consists of three sections; the first section will focus on formation damage, retention sites and retention mechanisms. The second one will give an overview about water quality and the different factors that affect it. The last section describes the forces that act on the particle in the colloidal system.

1.1. Formation Damage

The concept of formation damage means that the texture of the rock matrix is adversely altered and causes a reduction in porosity and permeability. It can also be defined as a reduction in permeability of the formation.

There are four mechanisms responsible for decline in well injectivity:

1. external filter cakes
2. internal filter cakes
3. wellbore fill-up
4. perforation plugging

Degree of impairment of porous medium depends on:

1. Suspended solids in the injected water
2. Injection rate
3. Particle Characteristics
4. Formation characteristics
5. Nature of interaction between particles and reservoir rock

Depending on the magnitude of these parameters, one of the following scenarios can occur:

1. Pure Internal Filtration
2. Pure External Filtration
3. Initial Internal Filtration followed by External Filtration
4. Initial Internal Filtration followed by simultaneously Internal and External Filtration

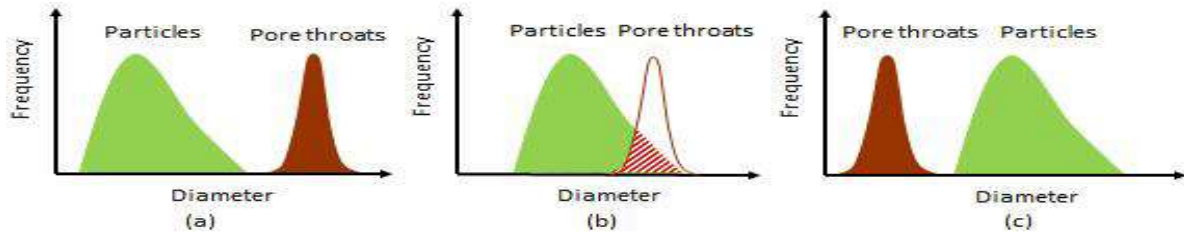


Figure 3: Particle and pore throat size distributions responsible for internal and external filtrations. (a) Pure internal filtration; Internal followed by external filtration (b) Simultaneous internal and external filtrations; (c) Pure external filtration.

1.2. Deposition Profile and Retention Sites

Deposition Profile:

The particles may deposit or they may be carried by the stream depending on magnitude of different forces responsible for deposition. Simultaneous arrival of particles towards the pore throat leads to formation of a particle bridge which in turn blocks the pore throats. The particles that are too large to pass through a pore throat are trapped in the constriction sites. Subsequently, the flowing particles accumulate at the bridge and completely block the porous medium. Straining in such a constriction may not be due to simultaneous arrival of particles but also due to successive stoppage of particles in a crevice site, where the particles are wedged between the convex surfaces of the grains. Deposition of particles can also occur in cavern sites; a small area formed by several grains. Another mechanism causing build-up of the cake is the transition from internal to external filtration by subsequent bridging of particles at the pore throats.

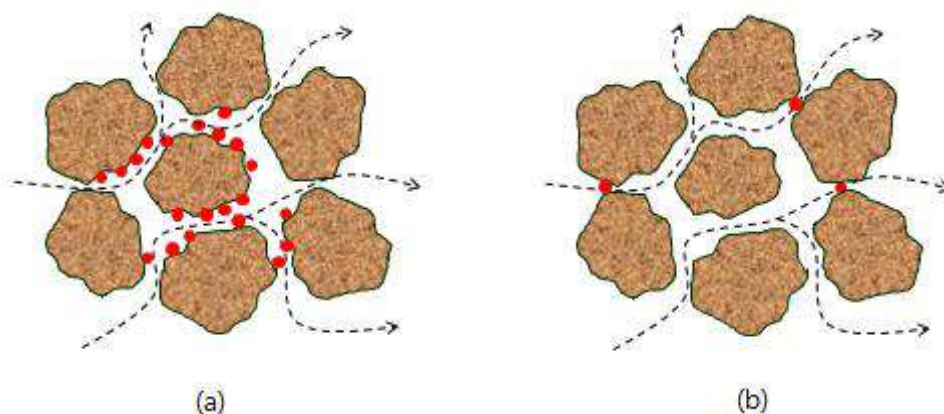


Figure 4: (a) Particle deposition on the rock surface; (b) Particle deposition in a constriction.

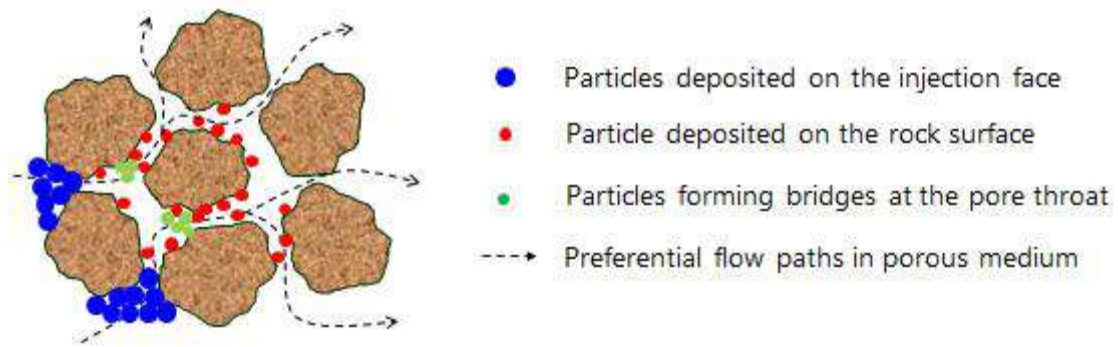


Figure 5: Porous medium depicting the formation of external filter cake on the injection face.

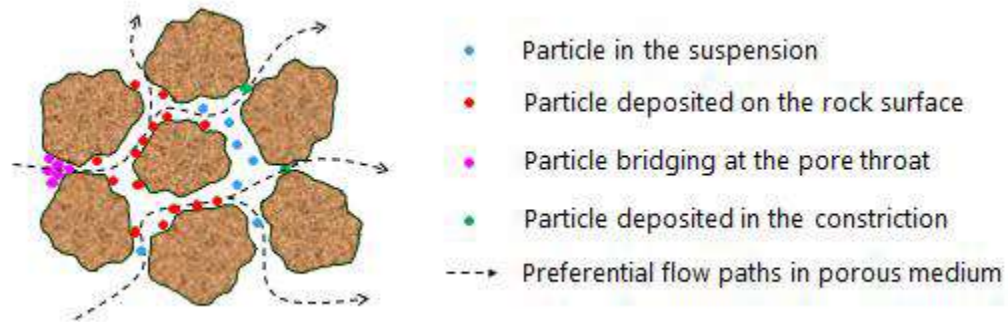


Figure 6: Porous medium depicting simultaneous occurrence of various mechanisms for deposition of particles.

Retention Sites:

1. Surface sites: surface of grains forming a porous medium.
2. Constriction sites: when space between grains are smaller than the size of particle.
3. Crevice sites: cleft or convex formed between multiple grains.
4. Cavern sites: sheltered area or small pockets formed by grains that are not disturbed by flow streams.

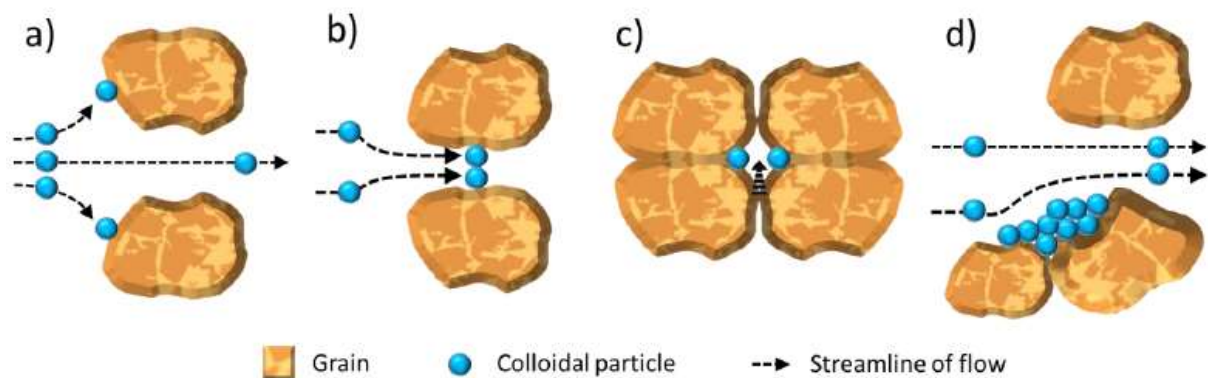


Figure 7: Retention sites in porous media a) Surface sites, b) Constriction sites, c) Crevice sites and d) Cavern sites

1.3. Retention Mechanisms

1. Sedimentation:

If there is density difference between the particle and the carrier fluid then sedimentation would take place. When the density of particles is different than the density of the fluid, the velocity of the particles will be different from the velocity of fluid and as result particles will deviate from streamlines. Therefore, particles will be subjected to gravity and get into the contact with grains.

2. Inertial Impaction:

As the porous medium is mostly torturous in nature, therefore, streamlines of the fluid flow change suddenly and a particle owing to its apparent weight tend to deviate from the streamline of flow and get in contact with the porous medium grains. When the density of particle is larger than that of the fluid, inertia forces will deviate the particle from the stream line and it may attach to the surface of a grain.

3. Direct Interception:

Particle following the stream line of flow hits a grain and gets retained. Interception happens when a particle following a streamline hits the surface of a grain and attaches to it. Particles with a density equal to the fluid density follow the streamline in the porous media, especially at low velocities. Eventually particles will be brought into contact with grain surfaces, because of the finite size of the particles.

4. Dispersion/Diffusion:

Particle might diffuse due to Brownian motion or disperse indirectly due to diffusion and reach areas that are not normally populated by them and get retained at a grain there. Small particles will be subject to random Brownian motion that increases the number of collisions between particles and grains. Diffusion is more important for small particles ($d_p < 1 \mu\text{m}$) and is usually neglected for larger particles.

5. **Surface forces (Electrostatic Deposition):**

Due to the difference in surface charge of the particle and rock, there would exist attraction or repulsion force. Van der Waals attraction and double layer repulsion are significant forces responsible for this type of retention mechanism.

6. **Straining:**

When a particle enters a throat that is too small for it to pass through, it gets stuck there. This phenomenon is called straining or size exclusion. The most critical factor determining straining within a porous medium is the ratio of the media (throat) diameter to the particle diameter. When this ratio is small it means that the throat size is too small for a particle to pass through. When this ratio is too small (less than 10) cake will be built up on the surface of the media.

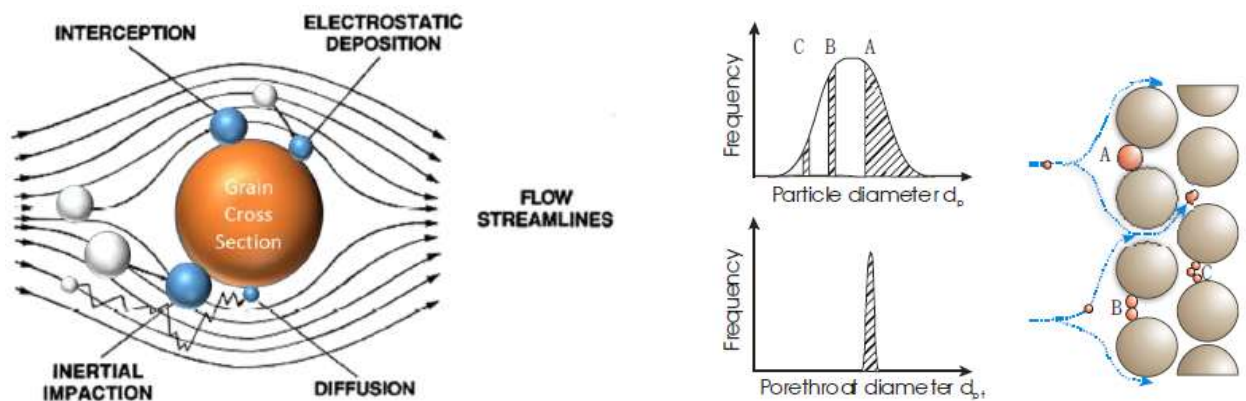


Figure 8: Illustration of particle retention mechanisms in porous medium

By looking at multiple collectors, three main retention mechanisms can be characterised i.e. surface deposition, plugging and entrapment.

1. **Surface Deposition:**

When particles get deposited at the surface of the grains of porous media, it is termed as surface deposition or adsorption.

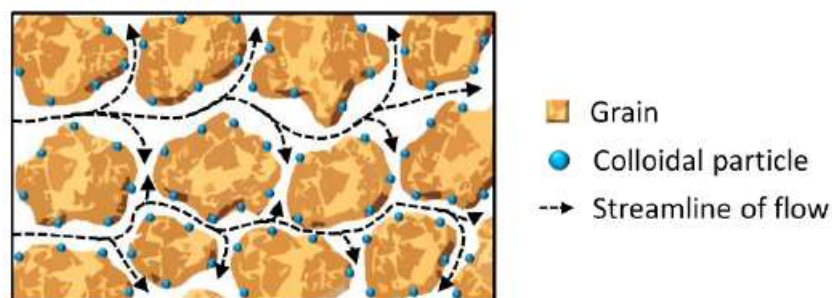


Figure 9: Surface deposition of particles in porous medium

2. Plugging:

If a single particle or collection of particles approach a pore throat smaller than their size at the same time then plugging would take place. Plugging with single particle is known as mono-particle plugging. Plugging with multiple particles it is termed as multi-particle plugging. Particles or fines dispersed in-situ can also form a bridge at pore throats in presence of salt over time. This type of plugging is called bridging.

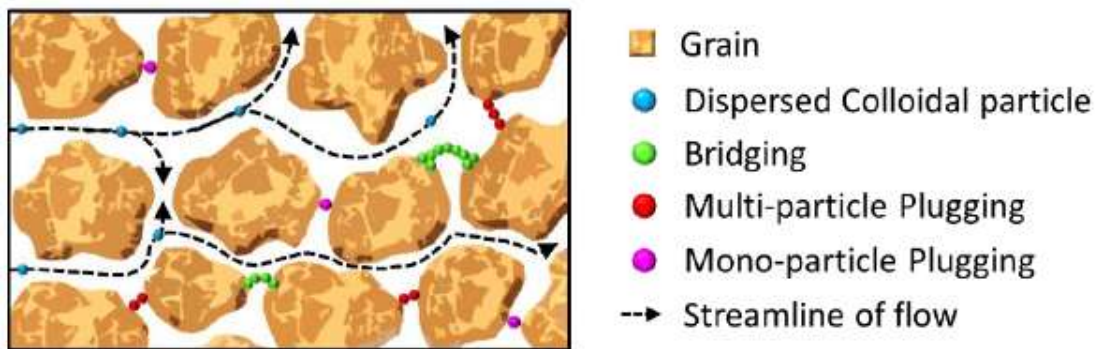


Figure 10: Illustration of bridging, multi –particle and mono-particle plugging in porous media

3. Entrainment:

Entrainment takes place when a deposited or plugged particle gets detached and is entrained by the flow into porous medium. Retention mechanisms described earlier make a porous medium to act as a filter when colloid is injected into it. Internal Filter Cake occurred when suspended or colloidal particles getting retained inside a porous medium is known as internal filter cake or deep bed filtration. However, external Filter Cake is a term used to describe the suspended and colloidal particles retained at the interface of a porous medium due to straining or size exclusion. External filter cake may be consolidated by the effect of fluid pressure as colloid flows through the cake.

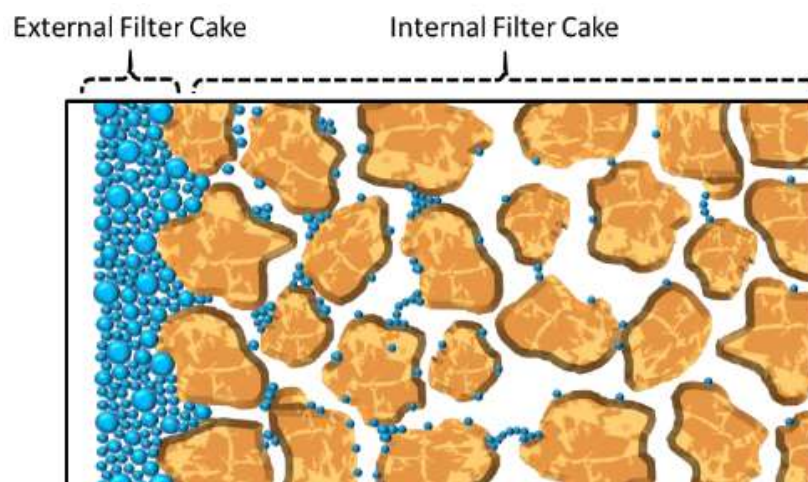


Figure 11: External and Internal filter cake

Based on the retention mechanisms mentioned earlier, impact of each retention mechanism was studied based on their collision probability with varying particle size:

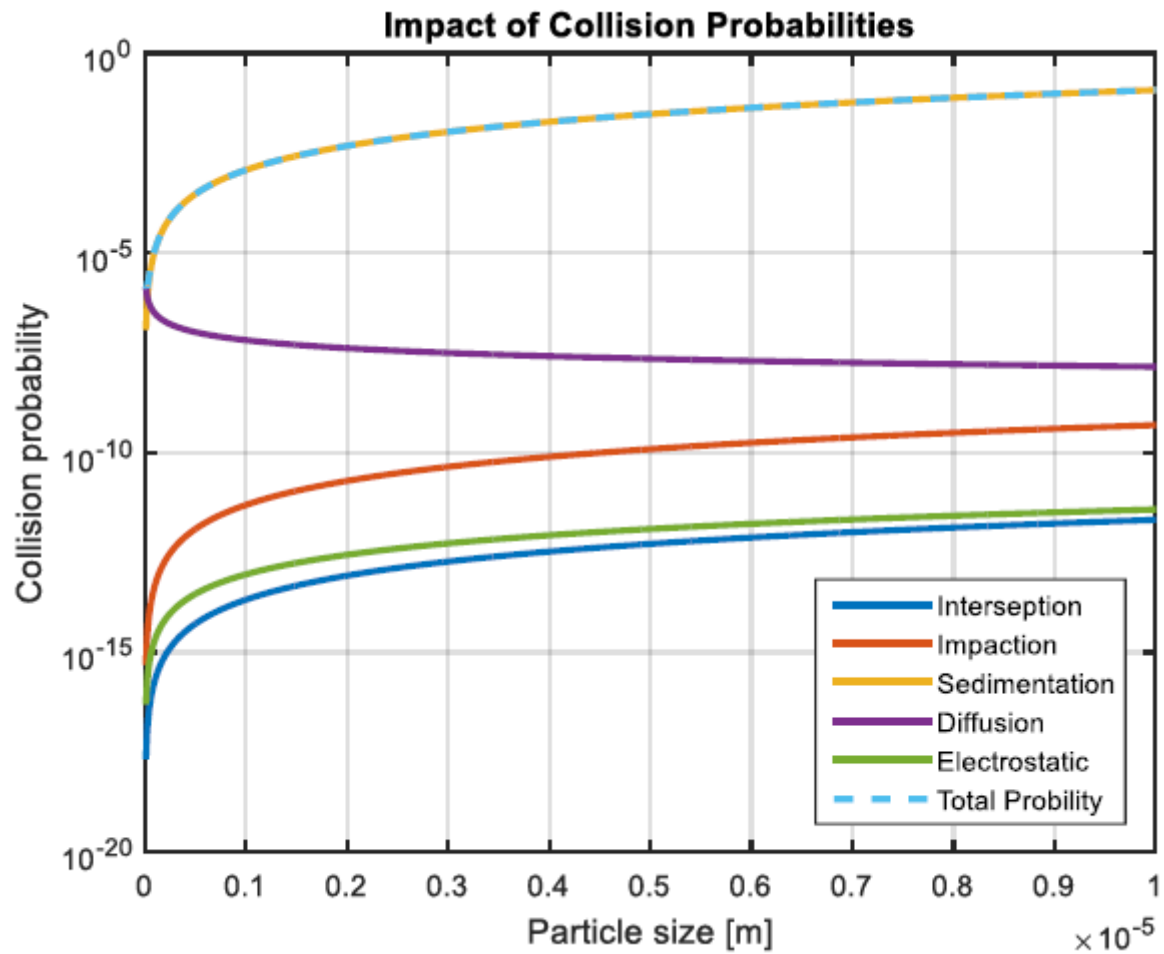


Figure 12: Impact of different capture processes on varying particle size.

We can notice from this graph that the probability of all the capture processes increases with the increase in particle size except for diffusion or dispersion which on the contrary has higher impact for particles less than $1\mu\text{m}$.

2. Water Quality

Water quality can be defined by three main factors:

- dispersed solid particles,
- dissolved salt concentration
- PH

In general salt concentration and pH of injection water could determine whether in-situ fines will be released from a potential source in the reservoir and also the likelihood of already dispersed solids to aggregate. This depends on the forces between the surface of the dispersed solids and reservoir grains. These inter-surface forces are subject to DLVO theory that is sum of London van der Waals attraction, double layer attraction or repulsion and short range forces.

2.1. Solid particles

Solid particles can be classified into two main categories:

colloidal particles	suspended particles
Biggest dimension with a size smaller than 1 μ m.	The biggest dimension with a size greater than 1 μ m.
The mixture prepared by using suspended particles is called suspension	The mixture prepared with colloidal particles is called colloid.
Colloidal particles are mostly invisible with say 0.5 μ m wavelength of ordinary light	Suspended particles can easily be observed by naked eye

Table (2-1): The difference between colloidal and suspended particles

Below particle size of 1 μ m, surface effects such as adsorption begin to predominate and as particle size decreases, colloidal interactions become increasingly significant relative to external forces (gravitational and hydrodynamic effects). In natural waters an operational distinction has been made between suspended and colloidal particles, if the particles get retained at a membrane filter of 0.45 μ m then they are suspended particles otherwise they are classified as colloidal particles. This operational distinction is commonly referred to as total suspended solid (TSS) limit.

2.2. Influence of Salt Concentration

When salt concentration of injection fluid exceeds a critical value, clay minerals present in the reservoir would swell. Swelling of clays results in increase in attractive forces between clay particles as their double layer is compressed due to part of the cations moves from the diffuse layer to the

stern layer. Consequently the zeta-potential decreases. This causes aggregation or bridging of clay particles to form bigger particles.

Fines attached to swelling clays may also dislodge and liberate while swelling of clays. The amount of swelling depends on the type of clay, for example montmorillonite (smectite group) swells more than illite or kaolinite (kaolin group). In terms of dispersed particles, salt concentration influences the double layer thickness and the stability of colloid.

2.3. Influence of pH

PH affects the stability of colloid as electric double layer of particles is altered by variation in pH which could result in increasing or decreasing zeta-potential. Reduction in magnitude of zeta-potential value reduces the repulsive forces between particles which results in formation of aggregates. PH could also influence release of fines by clay dispersal and by dissolution of cementing agents such as oxide minerals and calcites. There is a characteristic PH value where the surface has no charge and is called point of zero charge (PZC). It is repeatedly reported in literature that if injection water's pH is high i.e. >9, then permeability reduction is experienced even in sandstones with little clay content.

2.4. DLVO Theory

DLVO Theory is the classical explanation of the stability of colloids in suspension. It looks at the balance between two opposing forces — Electrostatic repulsion and Van-der Waals attraction — to explain why some colloidal systems coagulate while others do not. When two similarly charged particles approach each other in an electrolyte solution then there exists repulsive force between them due to overlap of their diffuse electric double layer. But in the same time there exists an attractive force between molecules that is known as London van der Waals forces. Sum of repulsive and attractive potentials curves give a net potential curve. If the net potential curve is repulsive then the highest value on this curve is called energy barrier. If the kinetic energy of particles on a collision course increases the energy barrier then they agglomerate.

2.5. Electric Double Layer

When a particle is dispersed in electrolyte, some of the counter-ions are electrostatically attracted close to the particle's surface and the rest remain randomly diffused throughout the solution. Negatively charged particle initially repels co-ions (anions) and attracts its counter-ions (cations) which form a firm layer around the surface of the particle.

This layer is known as Stern layer. Other counter-ions are still attracted by the particle but due to the formation of stern layer, these counter-ions are repelled at the same time too. This results in formation of diffuse layer of counter-ions. The concentration of counter-ions reduces whereas concentration of co-ions increases further away from the particle, till it reaches equilibrium with solution's concentration. The surface charge on a particle and associated counter-ion charge in stern and diffuse layer altogether form an electric double layer.

2.6. Zeta Potential (ζ)

Most widely used experimental technique to study the surface charge is through electro-kinetic techniques. Whenever there is a relative movement between a charged particle and electrolyte solution, part of double layer charge moves with the liquid. The concept of plane of shear distinguishes between the fixed and mobile parts of electric double layer. The electrical potential at shear plane is known as electro-kinetic potential or zeta potential. Shear plane is known to lie outside but fairly close to stern plane indicating all of diffuse layer is mobile whereas counter-ions in stern layer are fixed. This highlights the fact that value of zeta potential is less than true surface charge but as there exists clear correlation between zeta potential and colloidal stability, this value is widely used.

2.7. Electrophoretic Mobility

The device used in this study to measure zeta potential is Malvern Zetasizer Nano-ZS.

This device uses the concept of electrophoresis where the charged particle moves relative to liquid under the influence of an applied electrical field. Charged particles in the solution are attracted towards the electrode of opposite charge. Viscous forces acting on the particles oppose this movement but when equilibrium is reached between these two forces, the particle moves with constant velocity. This velocity is commonly known as electrophoretic mobility and is related to the zeta potential of the particle, viscosity and dielectric constant of the liquid by Henry's equation.

3. Forces Acting On a Particle In a Colloidal System

The main forces that act on the particle in the colloidal system are:

- Drag forces
- Lift forces
- Net Gravity force
- Interparticle forces
 - i. Electrostatic Interactions
 - ii. Van der Waals Forces
- Diffusion
 - i. Brownian Diffusion
 - ii. Shear induced diffusion
- Friction Force

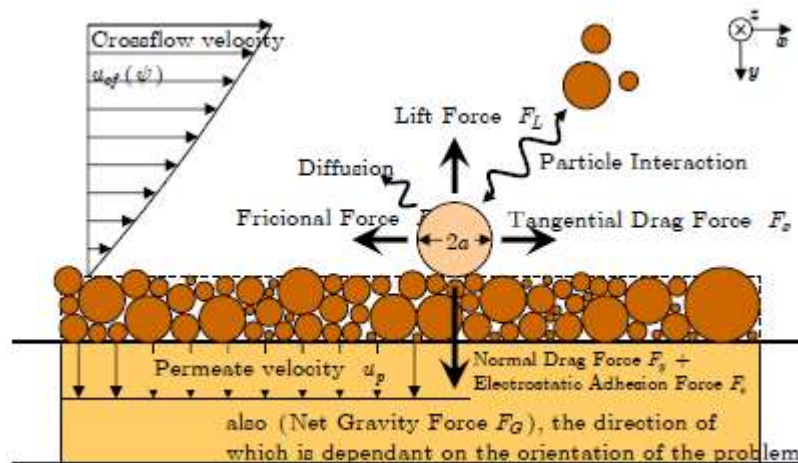


Figure 13: Schematic of the forces acting on a particle in the cake surface in a crossflow filtration process

3.1. Drag Force

Drag is the component of the force acting on a body parallel to the opposite direction to motion.

In colloidal systems drag forces arise due to the resistance of surrounding fluid to the motion of particles. The resistance is caused by the viscous shear of the fluid flowing over the particles and by the pressure difference between the upstream and downstream sides of the moving particle.

The viscosity of the suspending fluid is a measure of the resistance of the fluid to particle motion. The drag force acts in a direction opposite to the particle velocity, thus opposing the particle motion.

3.2. Lift Force

In a colloidal system lift force is caused by the shear flow. Lift force is a consequence of the velocity gradient. When the fluid reaches particle it is believed that velocity on top of the particle is higher than in bottom part. Lift force induced by shear flow is always perpendicular to drag force caused by that velocity. It is in the direction of permeate flow.

3.3. Net Gravity Force

Buoyancy force results from the density difference between particles and the fluid in the suspension. Depending on the magnitude of particle density, buoyancy can act vertically upwards or vertically downwards. If the density of particle is higher than the density of fluid the force will act in vertically upward direction. If the density of particle is less than the density of fluid the buoyancy will act in vertically downward direction.

3.4. Interparticle forces

1. Electrostatic Interactions
2. Van der Waals Forces

Electrostatic Interactions:

The electrostatic repulsions between the particles create an energy barrier that prevents the coalescence of the particles. However, the electrostatic interaction between charged colloidal particles involves not only the interactions between the colloidal particles, but also the interactions between colloidal particles and the sea of ions surrounding the particles. As every particle has a finite surface charge there should be an excess of ions of opposite charge in the solution to maintain overall electric neutrality of the system (DLVO theory 1942). Oppositely charged ions in the system are attracted towards the ions present on the surface of particles. But the thermal motion of the ions counteracts this attraction. Therefore, the ions take an equilibrium position to balance the electrostatic interaction energy with the thermal energy. This results in a diffuse double layer of ions surrounding the particle: one layer formed from the charge on the surface of the particles and other layer form from excess of oppositely charged ions present in the solution.

Van der Waals Forces:

Van der Waals attractive forces are weak forces that exist between uncharged molecules as a result of polarity. These forces become significant when sizes of the particles are very small and the distances are in nano level.

3.5. Diffusion

1. Brownian Diffusion
2. Shear induced diffusion

Brownian Diffusion:

In crossflow filtration permeate flux drags particles towards the filter medium, but from the other side the crossflow induces particles back transport into the bulk. Diffusion of the particles helps to the back transport of the particles.

Shear induced diffusion:

Shear induced hydrodynamic diffusion of particles occurs because individual particles undergo random displacements from the streamlines in a shear flow as they interact with and tumble over other particles.

3.6. Friction Force

Coulomb conducted hundreds of experiments with different material in broad range of conditions. He found out that the magnitude of frictional force is proportional to the sum of normal forces.

Chapter Three: Brine Characterization

This chapter includes all the characterization studies that have been done on brine in order to study the stability of the suspended solid particles in water and to determine the optimum conditions of salinity, PH and suspended solid particles size and concentration at which the effect of flocculation and coagulation is very low. The first stage of the characterization phase was the selection of the size and the type of the suspended solid particles that are going to be used in all tests and experiments. The next stage of the characterization phase was to study the effect of salinity on the average particle size distribution. The third stage was to study if the brine PH has an effect on the average particle size distribution. In the last stage, several brine samples with different suspended solid particles concentration have been prepared and tested to understand if the suspended solid particles concentration has also an effect one the average particle size distribution. By the end of this chapter a certain range of brine salinity, PH and suspended solid particles size and concentration were selected to be used in the second part of this research (core flooding experiments).

3.1 Selection of Suspended Solid Particle

Particle size is one of the most important factors that affect the water quality which in turn affect the decline in injectivity. Therefore studying the stability of particles in brine is mandatory before starting with core flooding experiments. Baracarb suspended particles are one of the common particle types that can be found in water. It is produced from ground marble with white powder or granules appearance. The chemical composition of Baracarb is Calcium Carbonate (CaCO_3 Calcium). It can resist size reduction beyond their specified range and have a specific gravity ranged from 2.7 to 2.78 g/cm^3 . It is an acid soluble that can be used as a bridging agent for fluid loss applications, increasing fluid density for drilling applications, or as part of a borehole strengthening treatment. It is available in seven particle size ranges from 2 to 1200 μm as shown in figure 14.

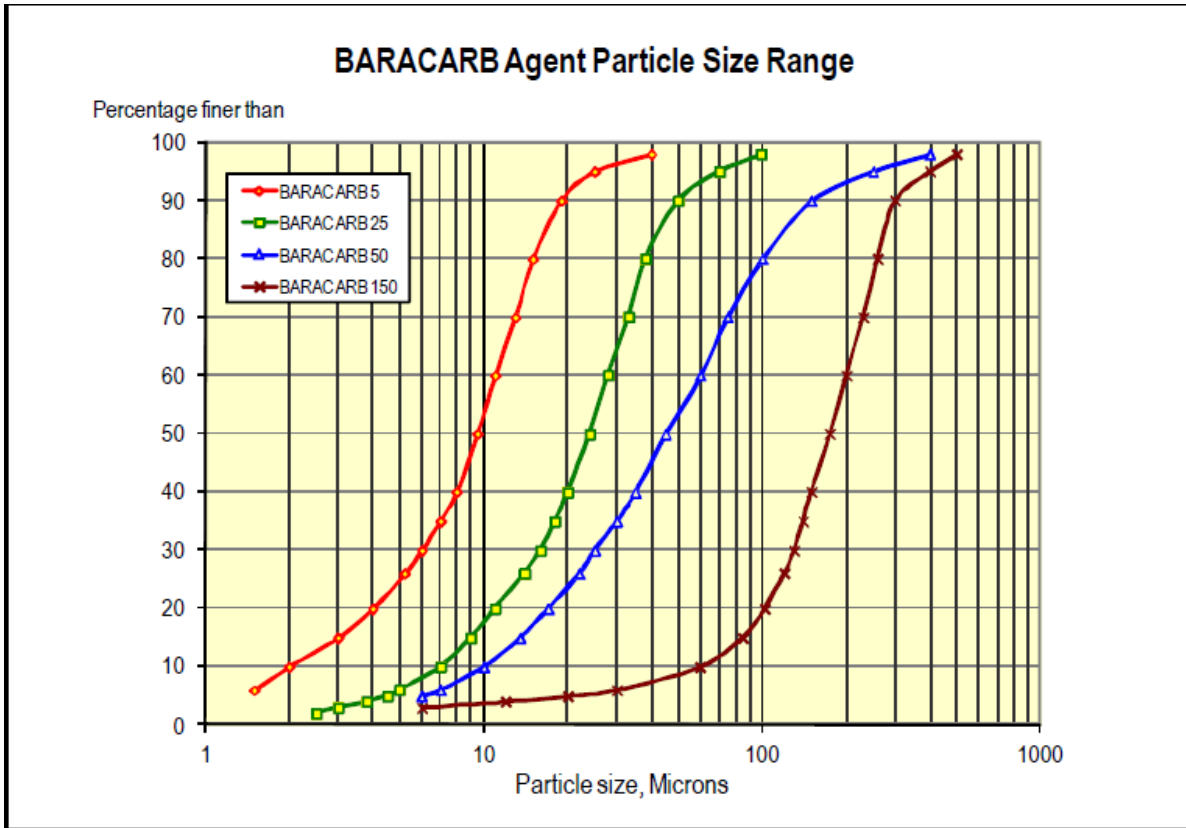


Figure 14: BARACARP particle size range according to HALLIBURTON product data sheet.

The selection of the suspended particle size that will be used through the characterization phase and after that in the core flooding experiments was based on the average pore diameter of Bentheimer sandstone, the type of rock that will be used in the core flooding experiments. Further discussion about the properties of the Bentheimer sandstone core plug will be in chapter five. The average pore diameter for Bentheimer sandstone from previous literature researches is 14 μm and the average pore throat diameter is 12 μm , as illustrated in figure 15. Based on this information, Baracarb of particle size 5 μm was selected to be used during the characterization experiments because it will be a good option to study both internal and external filtration during core flooding experiments.

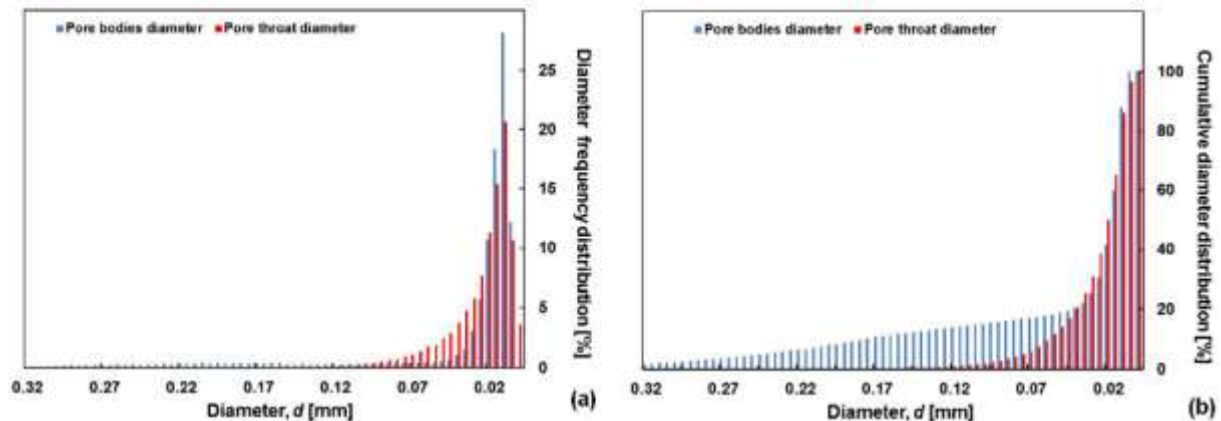


Figure 15: (a) Pore bodies and throats diameter frequency distribution; (b) Pore bodies and throats cumulative diameter distribution.

3.2 The Effect of Brine Salinity:

Selection of brine was not made randomly, but it was representing the composition of sea water that is used for injection projects. The exact composition of synthetic seawater brine is given in table (3-1). Different samples of brine with different salinity concentration were prepared. To detect the size of suspended Baracarb solid particles and particle size distribution, these samples were analysed using Bluewave Microtrac Particle Size Analyzer. This device provides accurate, reliable, and repeatable particle size analysis for a diverse range of applications by utilising the proven theory of Mie compensation for spherical particles and the proprietary principle of Modified Mie calculations for non-spherical particles.

Brine Composition	
Concentration	34179 [PPM]
Cations [PPM]	
Na⁺	10543
K⁺	388
Mg⁺	1243
Ca⁺	382
Anions [PPM]	
Cl⁻	18910
So₄⁻	2713
Salts [g/L]	
NaCl	23.50
KCl	0.74
MgCl₂ . 6 H₂O	10.40
CaCl₂ . 2 H₂O	1.40
Na₂SO₄ . 10 H₂O	9.10

Table (3-1): Synthetic seawater brine composition

The Bluewave Microtrac Particle Size Analyzer has tri-laser and allows light scattering measurements to be made from the forward low angle region to almost the entire angular spectrum (0.2 to 165 degrees). It does so by a combination of three lasers and two detector arrays, all in fixed positions. The primary laser (on-axis) produces scatter from nearly on-axis to about 60 degrees, detected by a forward array and a high-angle array, both of which have logarithmic spacing of the detector segments. The second laser (off-axis) is positioned to produce scatter beyond the 60 degree level which is detected using the same detector arrays. The third laser (off-axis) is positioned to produce backscatter, again using the same detector arrays.

This technique effectively multiplies the number of sensors that are available for detection of scattered light. Laser beam interacts with mixture of particle sizes where Light is scattered and the scattered light is then collected by a Fourier lens as shown in figure (). The Fourier lens focuses the light onto a silicon detector where the detector responds to light by producing a series of voltages. These voltages represent signals that produce a pattern that is a fingerprint. An Algorithm is used to calculate the volume percentage as a function of particle size.

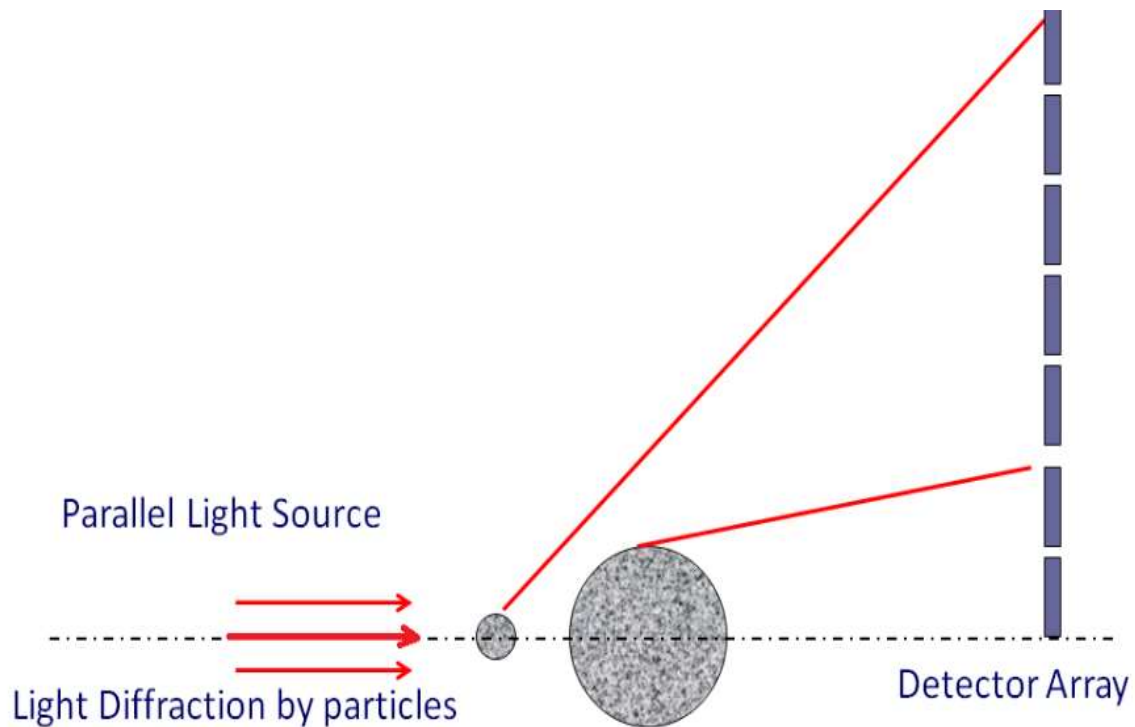


Figure 16: Schematic view of the light scattering technique used by Bluewave Microtrac Particle Size Analysis

The measurements obtained for all samples using the Bluewave Microtrac Particle Size Analyzer represent the average particle size and each value is an average of multiple runs. The characterization of the samples that were prepared for this test is given in table (3-2).

Sample No.	Salt Conc. [PPM]	PH	Particle Conc. [PPM]
SA-01	34179	8.3	100
SA-02	35888	8.2	100
SA-03	37597	8.2	100

Table (3-2): Properties of the samples prepared for the salinity test

The average particle size and the particle size distribution of the three samples were as following:

A. SA-01

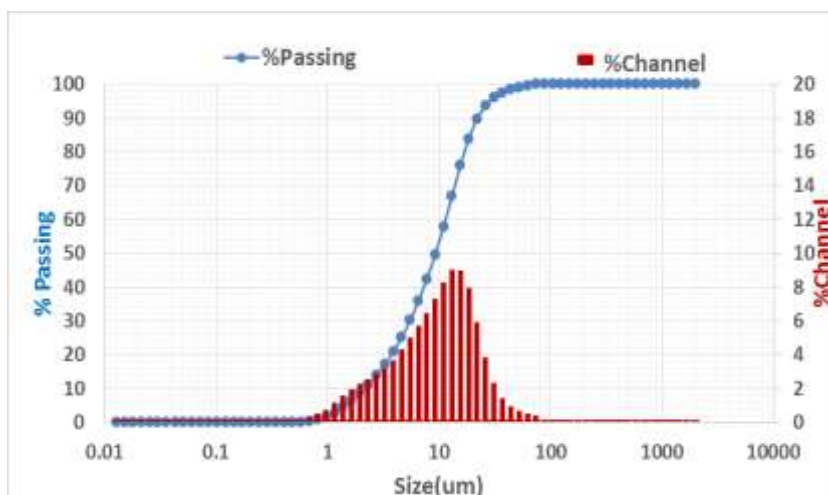


Figure 17: Average Particle Size Distribution for sample SA-01

B. SA-02

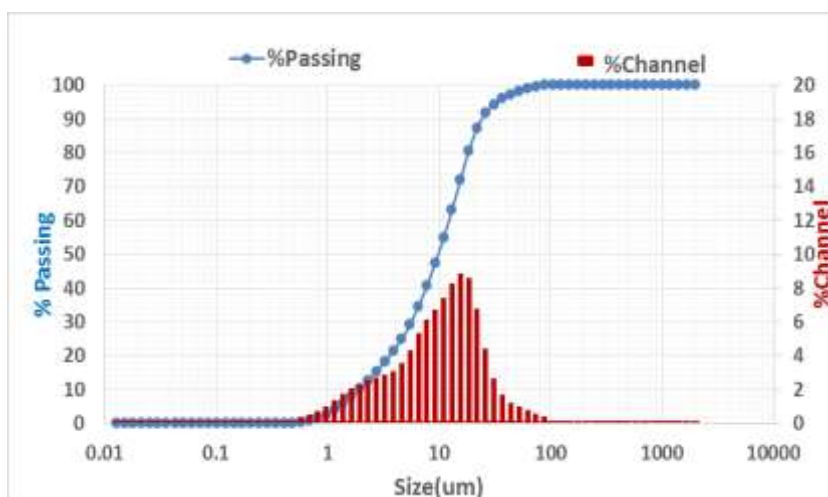


Figure 18: Average Particle Size Distribution for sample SA-02

C. SA-03

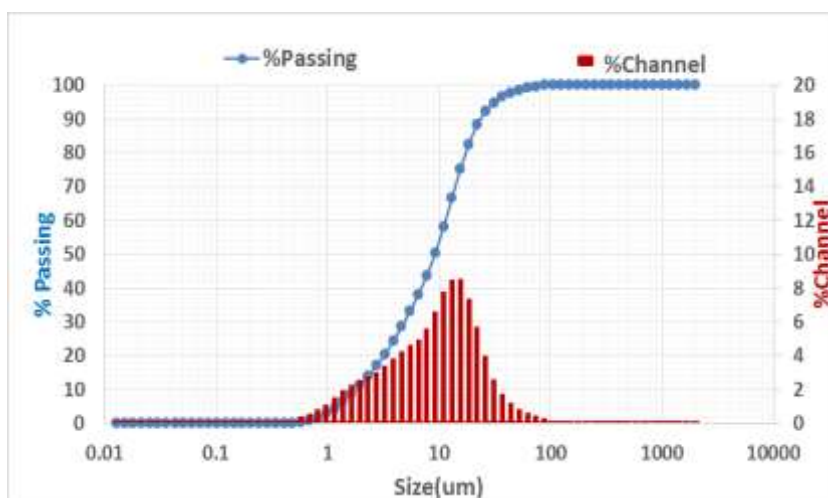


Figure 19: Average Particle Size Distribution for sample SA-03

From the obtained results, two observations were made. The first observation is that the hydrodynamic particle size of Baracarb solid particles in different brine samples is larger than 11.5 μm , although the size of the used particles was 5 μm . The second one is that by increasing the salinity, the hydrodynamic particle size of Baracarb solid particles increase as shown in figure (20).

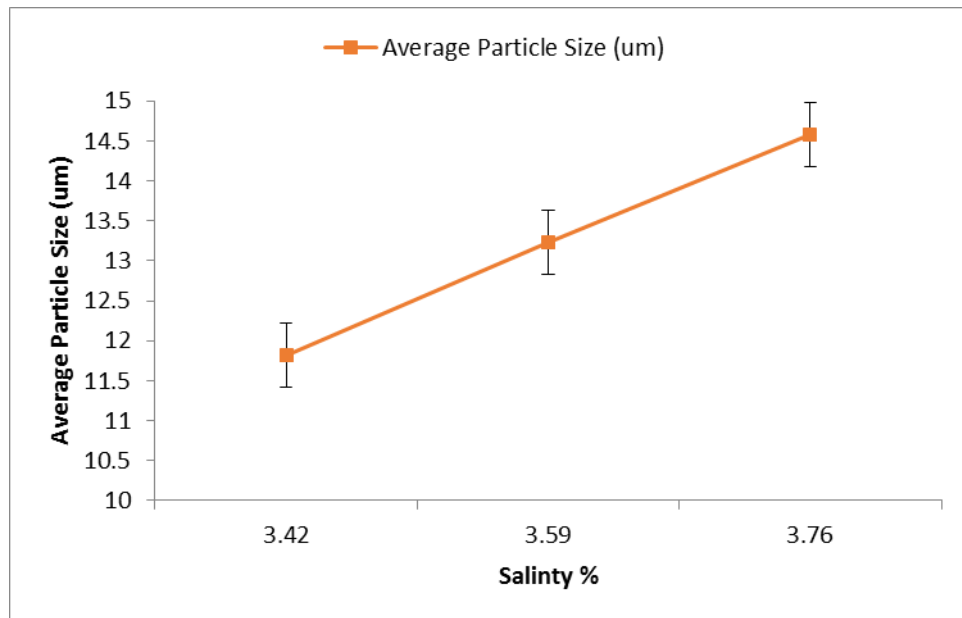


Figure 20: Data represent the effect of salinity on the average particle size.

3.3 The Effect of PH:

In order to study the effect of PH on the average particle size and the average particle distribution, different brine samples with different PH values have been prepared to be tested on the Bluewave Microtrac Particle Size Analyzer. The characterization of the samples that were prepared for this test is given in table (3-3).

Sample No.	Salt Conc. [PPM]	PH	Particle Conc. [PPM]
SA-01-PH-07	34179	7.02	100
SA-01-PH-08	34179	8.17	100
SA-01-PH-09	34179	9.02	100

Table (3-3): Properties of the samples prepared for study the effect of PH on average particle size

The average particle size and the particle size distribution of the three samples were as following:

A. SA-01-PH-07

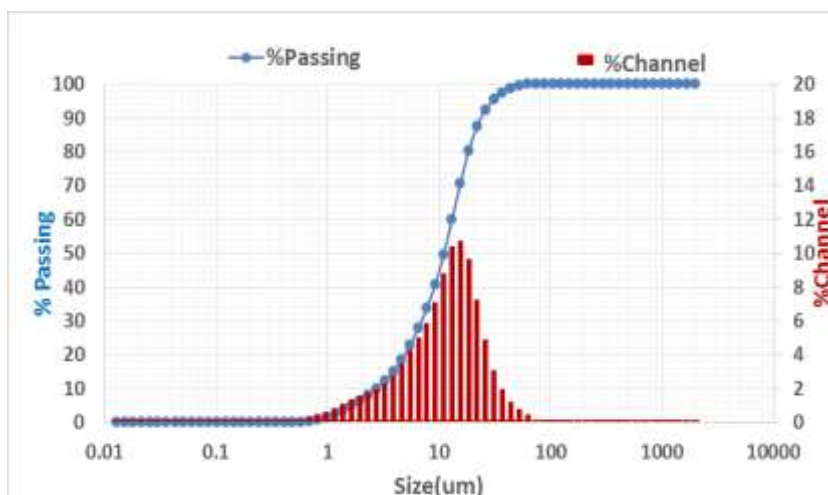


Figure 21: Average Particle Size Distribution for sample SA-01-PH-07

B. SA-01-PH-08

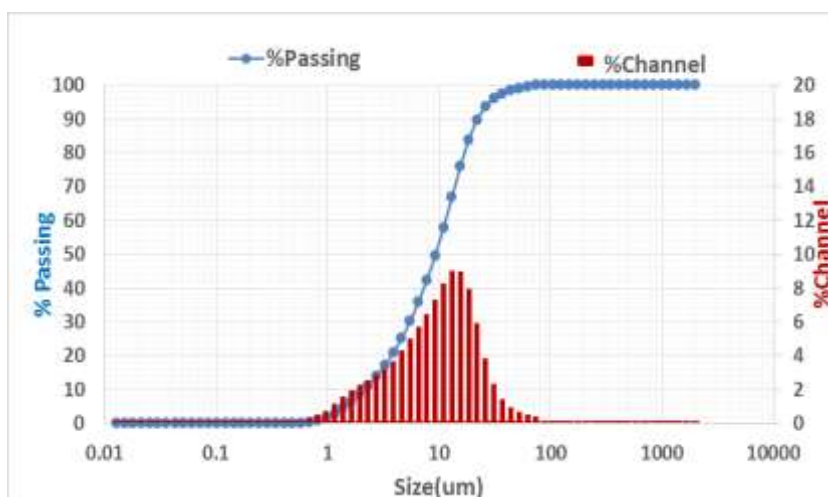


Figure 22: Average Particle Size Distribution for sample SA-01-PH-08

C. SA-01-PH-09

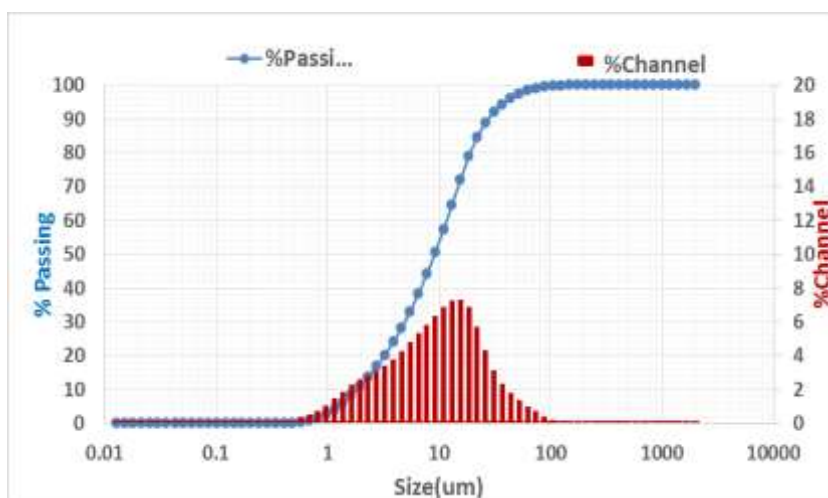


Figure 23: Average Particle Size Distribution for sample SA-01-PH-09

From the obtained results, the lower value of the hydrodynamic average Baracarb particle size in the brine was observed at a certain PH value of 8. However the average Baracarb particle size starts to increase rather higher than or lower than this PH value as shown in the figure ().

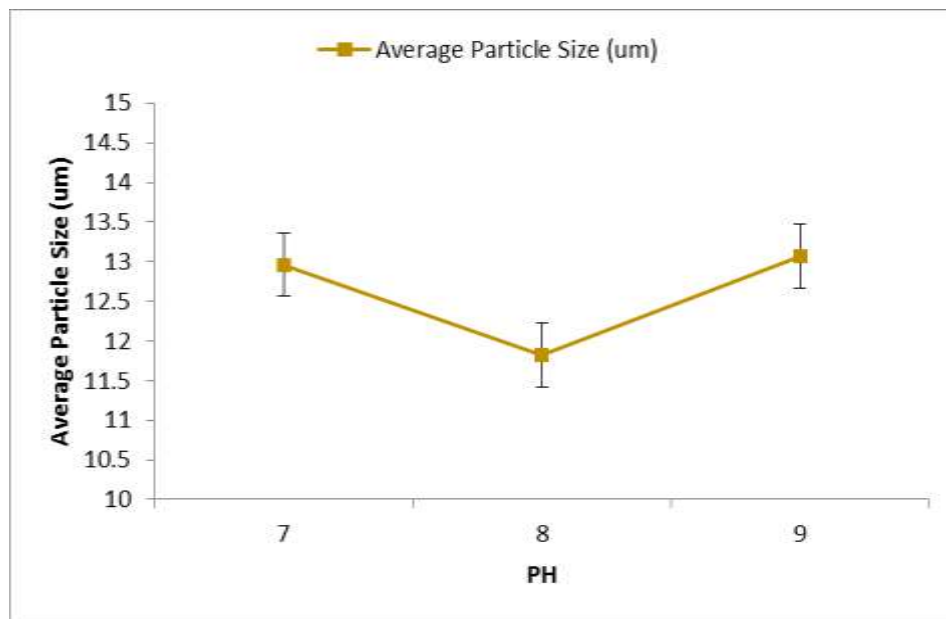


Figure 24: Data represent the effect of PH on the average particle size

3.4 The Effect of Particles Concentration:

The last step of the characterization phase was to change the suspended Baracarb solid particle concentration in the brine at constant salinity and PH and study its effect on the average particle size and the average particle distribution. The characterization of the samples that were prepared for this test is given in table (3-4).

Sample No.	Salt Conc. [PPM]	PH	Particle Conc. [PPM]
SA-01-PPM-50	34179	8.20	50
SA-01-PPM-100	34179	8.17	100
SA-01-PPM-250	34179	8.07	250
SA-01-PPM-500	34179	8.11	5000
SA-01-PPM-1000	34179	8.16	1000

Table (3-4) Properties of the samples prepared to study the effect of particle concentration on the average particle size.

The average particle size and the particle size distribution of the five samples were as following:

A. SA-01-PPM-50

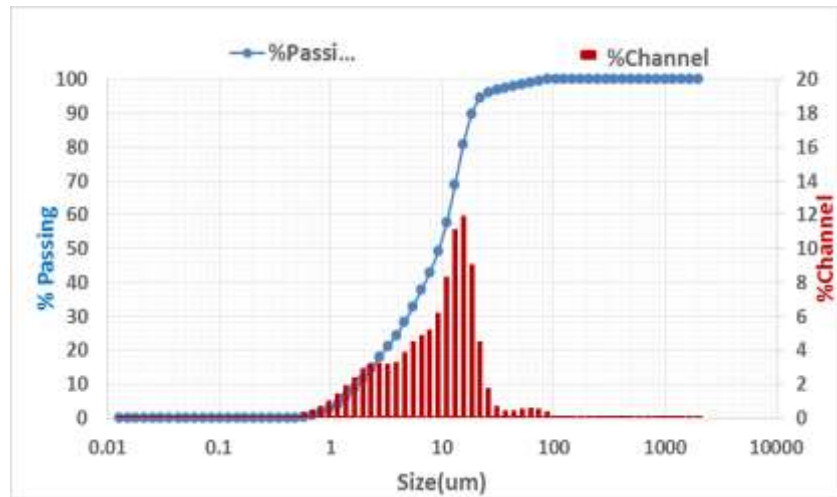


Figure 25: Average Particle Size Distribution for sample SA-01-PPM-50

B. SA-01-PPM-100

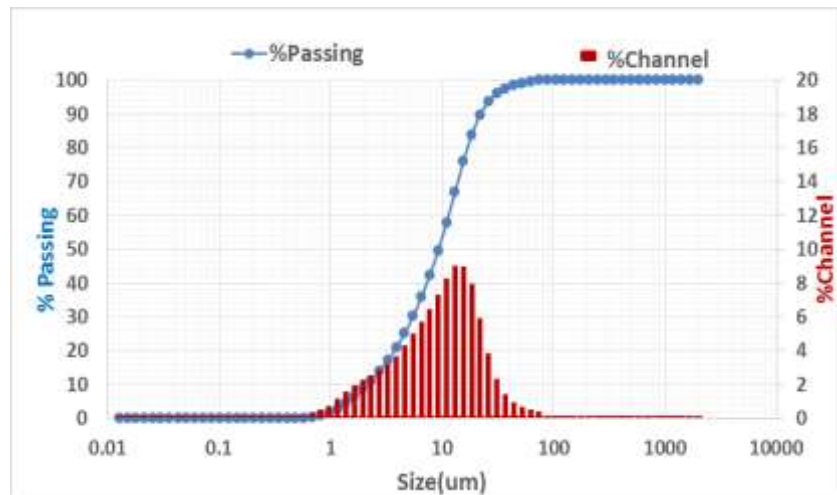


Figure 26: Average Particle Size Distribution for sample SA-01-PPM-100

C. SA-01-PPM-250

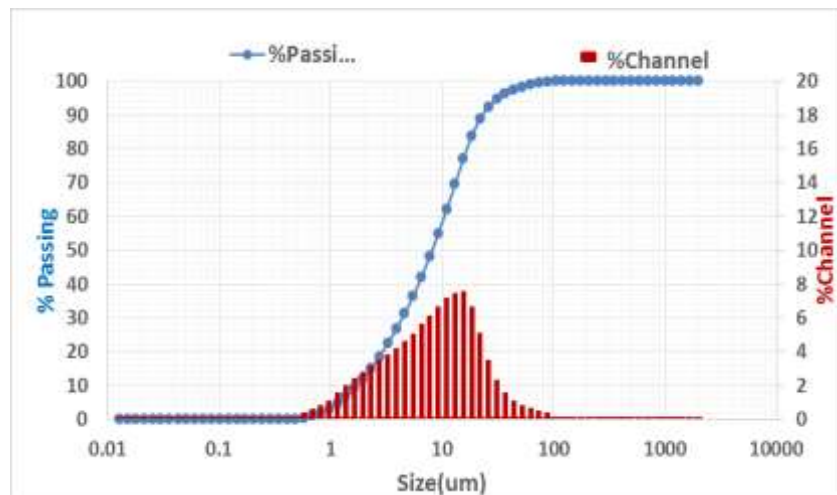


Figure 27: Average Particle Size Distribution for sample SA-01-PPM-250

D. SA-01-PPM-500

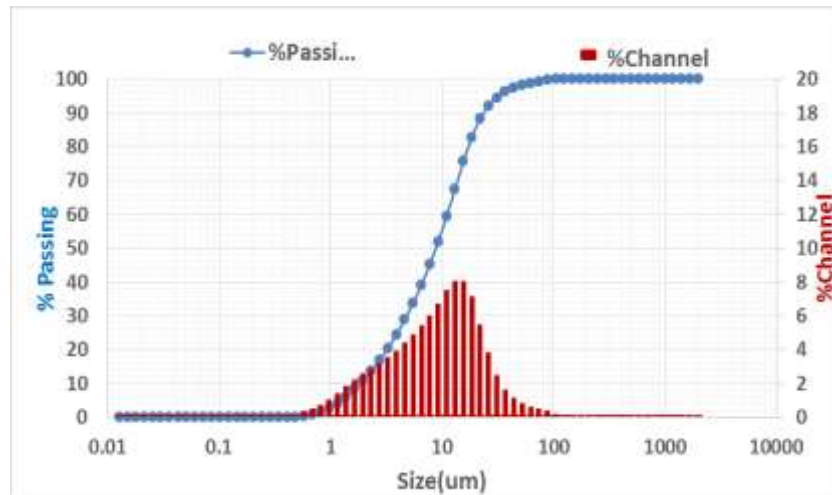


Figure 28: Average Size Particle Distribution for sample SA-01-PPM-500

E. SA-01-PPM-1000

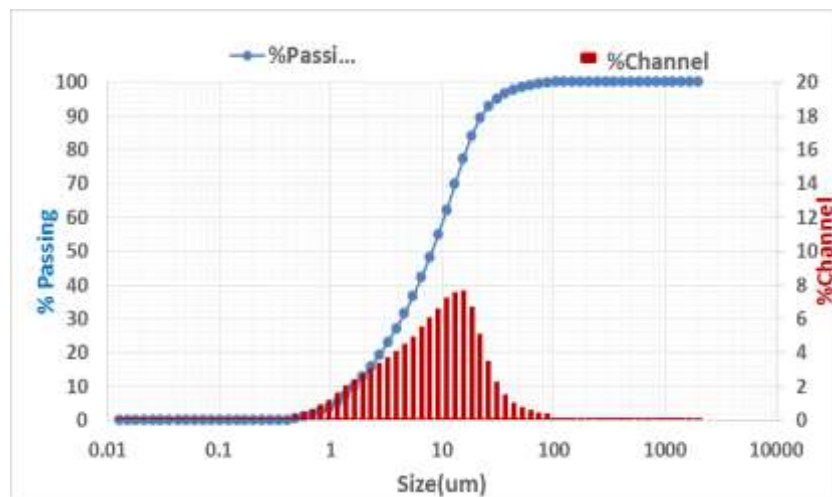


Figure 29: Average Particle Size Distribution for sample SA-01-PPM-1000

It can be observed from the obtained results that the concentration of suspended Baracarb particles in brine has no effect on both average particle size and the distribution of particle size as shown in figure (30).

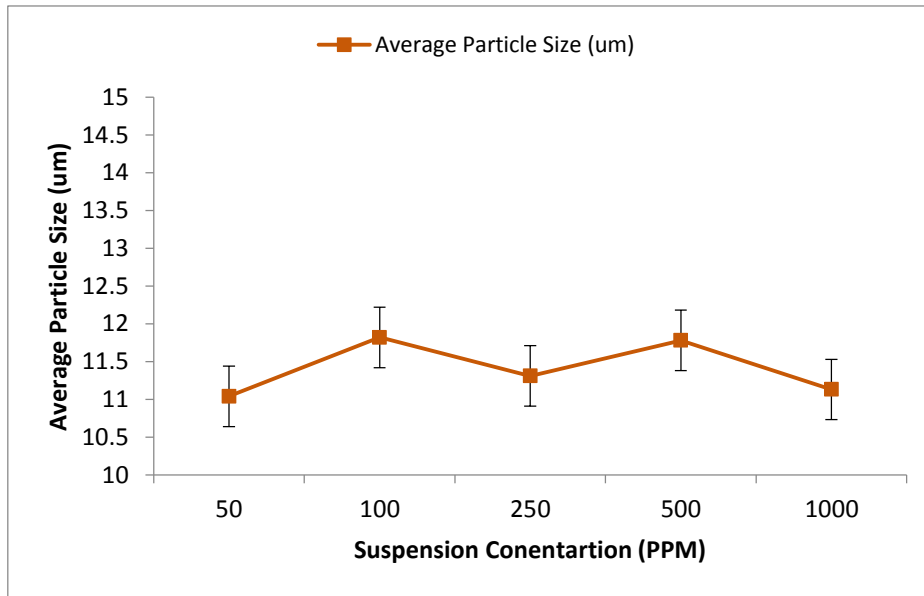


Figure 30: Data represent the effect of particle concentration on the average particle size

By the end of the characterization phase, we can summarize all the results that we have in four main points. The first point is related to the size of the Baracarb suspended solid particles used in all experiments. Although we use 5 μm Baracarb particles size, the hydrodynamic particle size of Baracarb particles in different brine samples is larger than 11.5 μm . The second point is the effect of brine salinity. As the brine salinity increase, the average particle size increase. The third point is that there is a specific PH range at which the lower value of the hydrodynamic average Baracarb particle size in the brine was observed. The last point declares that the concentration of Baracarb particles in brine has no clear effect on the hydrodynamic average particle size. Therefore, it was recommended to use 2 μm particle size instead of 5 μm in core flooding experiments to avoid the early formation of external filter cake. The brine used for core flooding experiments will have the salinity of 3.42%% and PH 7.

Chapter Four: Experiments

Core flood experiments were conducted using Baracarb 2 μm particles at different concentrations and flow rates to understand the formation damage mechanism during the flow of these particles through sandstone rock at core scale. Bentheimer sandstone core plugs were cut, dried and covered with yellow glue to be fit in the core holder. Absolute permeability tests were conducted using tap water then filtered brine prior to every experiment for each core plug. In this section, the preparation of the core plugs is presented along with core flood experimental setup, procedure and post-experiment analysis.

4.1 Characterization of the Porous Medium:

Bentheimer sandstone core plug was selected as a porous medium in the core flooding experiments. These rocks have good lateral continuity and exhibit block scale homogeneous nature. This sandstone block comes from the Romberg quarry in Gildehaus, Germany. It is an Aeolian deposit rock that shows constant mineralogy and is largely free of paramagnetic impurities, well consolidated and has well-sorted grain framework and pore network. It is composed of more than 90 % quartz, less than 3 % clay and less than 5 % feldspar with some traces of carbonate and oxide minerals. The exact composition is mentioned in the Table (4-1).

Mineral	A.E. Peksa et al. (2015) [wt%]	Maloney et al. (1990) [wt%]
Quartz	91.7	97.5
Clay	2.68	.5
Feldspar	4.86	2
Other	0.76	Traces
Sum	100	100

Table (4-1): XRD results of Bentheimer sandstone from literature

4.2 Core Plug Preparation:

Cylindrical cores were drilled out of large cubical block of specific diameter. Then they were sawn to desired dimensions with an accuracy of $\pm 1\text{mm}$. After that they were dried in an oven at a temperature of 60°C to remove water content and moisture. Afterwards, they were placed in the molds and coated with self-hardening glue. The purpose of this glue is to preserve the core and to ensure that when the core plug is placed in the core holder, the O-rings can be placed properly on glue to make the annular space between the core and core holder completely independent from the inlet. After hardening of the glue, excess glue is machined so that the core plug fits in the core

holder precisely. For the intermediate pressure data along the core, three holes were drilled in the core as shown in Figure (31). These holes were drilled at 0.8 cm, 7.18 cm and 13.56 cm respectively from the injection face. The core specific parameters are listed in table (4-2).

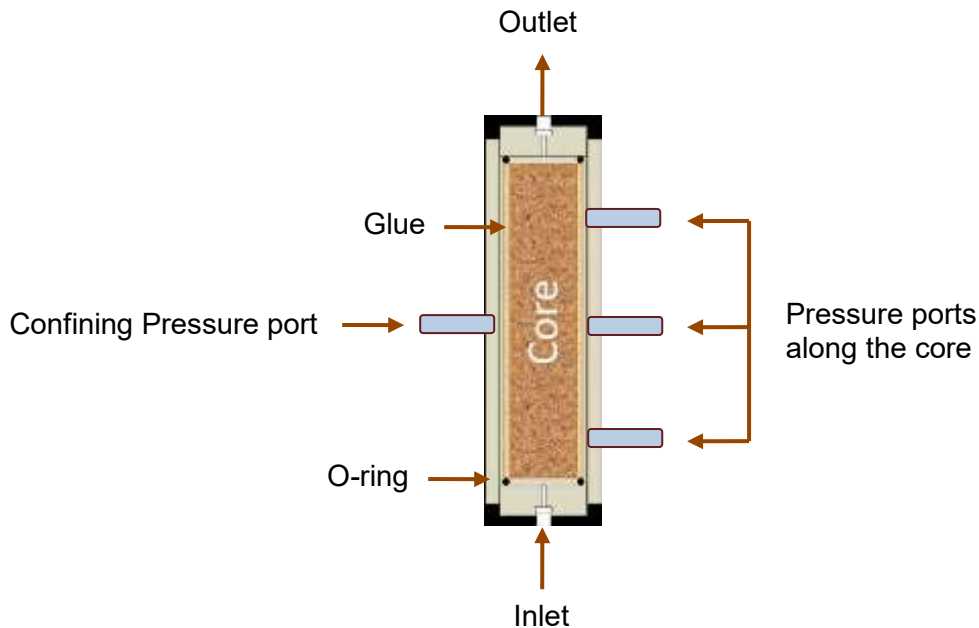


Figure 31: Schematic view of the core holder and core plug

Length	15.75 (cm)
Diameter	3.85 (cm)
X-section Area	11.64 (cm ²)
Pore Volume	46.02 (cm ³)

Table (4-2): The core specific parameters

4.3 Experimental Set up:

Experimental setup was designed and built in the reservoir engineering lab at Delft University of Technology. Setup comprised of various parts that are discussed in this section. The overall pressure rating of the experimental setup was 40 Bar. The schematic view of the experimental setup is shown in figure (32).

4.3.1 Injection Pump

An injection pump was used for the injection of water into the system for cleaning and flushing the system before and after each experiment. It is also used for the injection of brine for core saturation and permeability test. Its main task is to inject the suspension solution during the core flooding experiments. Quizix-QX pump was used for all experiments and it had flow rate accuracy of $\pm 0.1\%$ of set point.

4.3.2 Core Holder

The core plug holder is made of Poly Ether Ether Ketone (PEEK). It has excellent mechanical property and it is transparent to X-rays. With core plug enclosed in hardened glue and encapsulated in PEEK core holder, the combination can withstand pressure up to 50 Bar and temperature up to 50°C. The core holder had three pressure ports and one confining pressure port, see Figure (31).

4.3.3 Pressure Sensors

Four pressure differential transducers were used to measure the pressure difference along each section of the core and two pressure sensors for absolute pressure measurements of the whole setup. One differential pressure transducer of ± 40 Bar rating was used to measure pressure difference along the inlet and outlet of the core. Three differential pressure transducers of ± 3 Bar rating were used to measure the pressure difference between specific points along the core (see figure). Inlet and outlet pressures were monitored using pressure sensors of ± 50 Bar rating. All pressure sensors and differential pressure transducers were calibrated prior to experiments and had an offset of ± 0.001 Bar and ± 0.01 Bar respectively about the set point. All pressure sensors and differential pressure transducers readings were recorded using data acquisition software 'MP3 Measure' developed by National Instruments.

4.3.4 Flowlines, Connections & Accessories

Flow lines of plastic tubing with pressure rating of 38 Bar were used for the setup. Swagelok fittings and valves were used in order to regulate the flow and for connections and sample points. Moreover, the setup had a CO₂ cylinder, vacuum pump, back pressure valve for applying back pressure and confining pressure of 25 Bar and N₂ cylinder to apply pressure on back pressure valve for initially saturating the core plug with brine prior to each experiment.

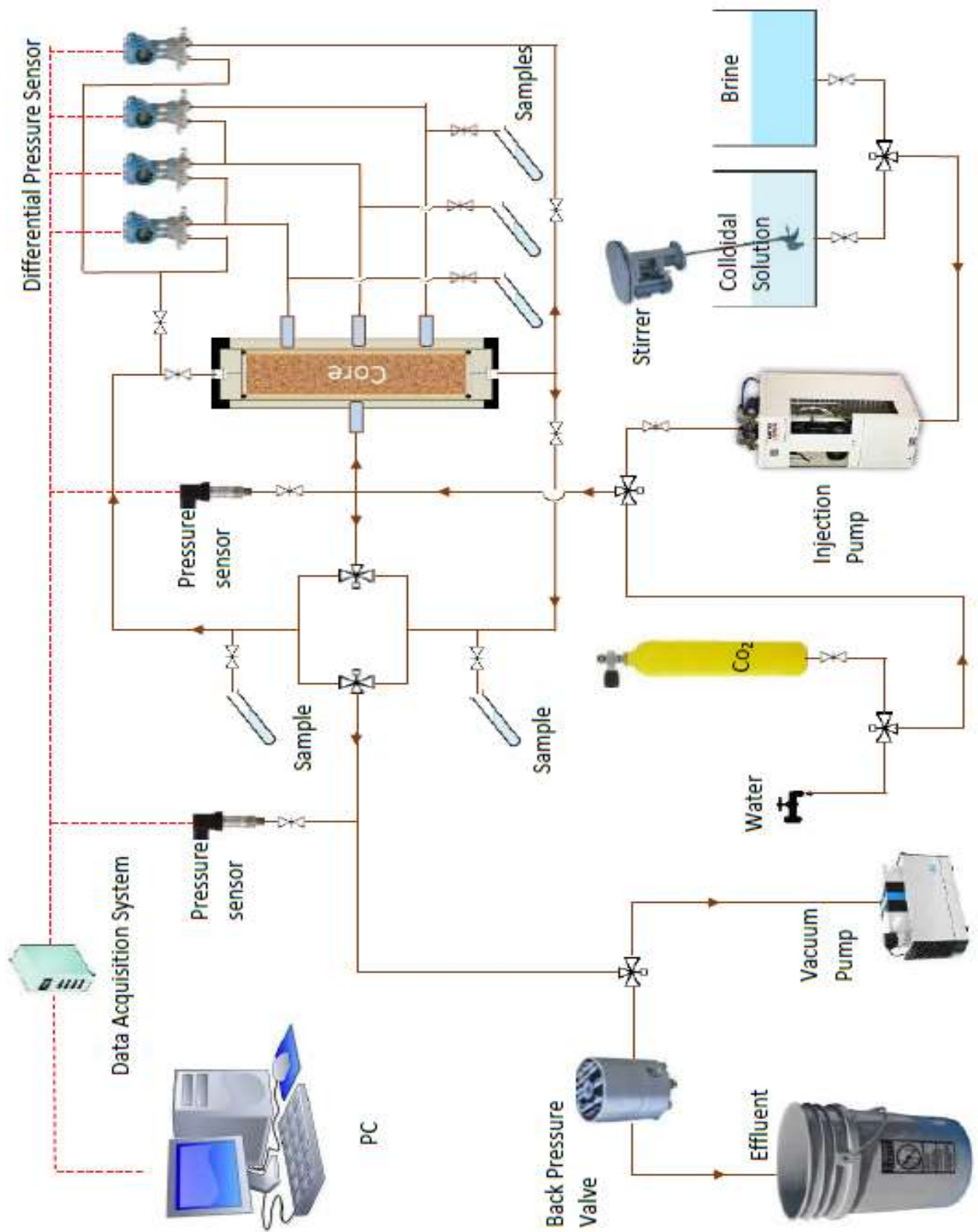


Figure 32: The schematic view of the experimental setup

4.4 Experimental Procedure:

- Prior to starting experiments, the cumulative dead volume of all flow lines, connections and valves shall be measured.
- The pump shall also be calibrated at different pump settings.
- All lines in the setup must be flushed with CO₂ to make sure no air is present in the lines.
- Then core holder containing the dry core plug is installed in the system and flushed with CO₂ at atmospheric pressure to remove trapped air from the core plug.
- The system is then pressurized to 2-3 Bar with He for a leak test. All connections shall be checked with snoop leak detection fluid. If a leak is observed, connections were remade.
- After ensuring no leak, the system is going to be vacuumed at -1 Bar to ensure no moisture or air remained in the system.
- After that vacuum was filled with CO₂ again, brine is injected into the system at by allowing the brine to enter the core from the bottom. This is done to ensure gravity stable condition so that no air bubble is formed in the core plug while saturation.
- Then the back pressure of 10 Bar will be applied while injecting brine to ensure complete saturation of core with brine.
- Once the core gets saturated, permeability tests can be conducted. Absolute permeability can be calculated by measuring pressure drop across the core at different flow rates.
- Then brine without silica particles is injected to observe any change in permeability due to brine.
- After this, suspension solution is injected into the core plug at a desired rate and a sample of injection fluid shall be taken at the inlet of the core plug to obtain the initial injection concentration of Baracarb particles.
- At the end of the experiment, all lines and pump shall be flushed by injecting fresh water through the system at high flow rates to remove any retained particles.

Chapter Five: Results and Discussion

Core flooding experiments were conducted on Bentheimer sandstone core plugs to study the effect of water quality on the injectivity decline. Tap water was initially injected which was followed by brine injection in all experiments to saturate the core. After the core has been saturated with brine, the injection of brine without particles continued to see if it would affect the core plug permeability. Then the Baracarp suspension solution was injected. In this section results obtained from these experiments are presented and discussed. The raw data obtained from experiments was pressure profile and colloidal influent/effluent concentration. Pressure data was used to obtain the injectivity decline for all experiments.

5.1 Permeability Measurements:

Absolute permeability was measured after saturating the core with water, and then using the same brine that was used for preparing suspension solution. Using Darcy's equation permeability was calculated. The plot of flow rate to area Q/A versus pressure difference per length $\Delta P/L$ was generated for each test. For Darcy's flow, data follows a straight line with a slope of k/μ . At high flow rates, turbulent flow is indicated by a deviation from the straight line but in all the tests, those high rates were never achieved.

The first segment of the core plug (i.e. ~0.8 cm) always showed relatively lower permeability in comparison to the other segments of the core. The reason for this mismatch could be due to the consequence of the sawing procedure of cutting the core plugs. Sawing core plugs to desired length results in damaging the face of the core plug which results in lower permeability of the first segment. The summary of the permeability measurements is mentioned in table (5-1).

Segment	Permeability (Darcy) (Tap Water)	Permeability (Darcy) (Brine)
Core	2.71	2.77
Segment 01	2.30	2.24
Segment 02	2.70	2.78
Segment 03	2.71	2.74

Table (5-1): permeability measurements using tap water and brine

5.2 Initial Brine Flow

Brine was injected before the suspension solution injection. The reason for injecting brine was to make sure that the rock properties do not change any further due to brine and rock interaction. It was observed that the absolute permeability of the core plugs increased further from what was calculated before. The extent of permeability increase was 3.6% (see Table 5-2). This increase of permeability could be due to the reduction of the clay swelling effect due to the high salinity of the brine. Permeability obtained at this stage was taken as initial permeability (k_0).

Segment	Permeability (Darcy) (After Brine Injection)
Core	2.87
Segment 01	2.28
Segment 02	2.86
Segment 03	2.88

Table (5-2): permeability measurements after brine injection (k_0)

5.3 Suspension Solution Injection

Once the initial permeability was obtained after initial brine injection, Baracarb suspension solution was injected. During the suspension flow, differential pressure was recorded along the core. These pressure measurements provided insight into deposition profile and overall injectivity decline. The flow parameters for the 1st core flooding experiment are mentioned in table (5-3).

Injection Rate	20 mL/min
Concentration	100 PPM
PH	8.1
Average Particle Size	2 μ m
Total PV Injected	910 PV
Duration	35 hrs

Table (5-3): flow parameters for the 1st core flooding experiment

5.4 Pressure drop profile

As mentioned before, during the suspension flow, differential pressure was recorded along each section of the core and along the inlet and outlet of the core. These pressure measurements are illustrated in the figure (33).

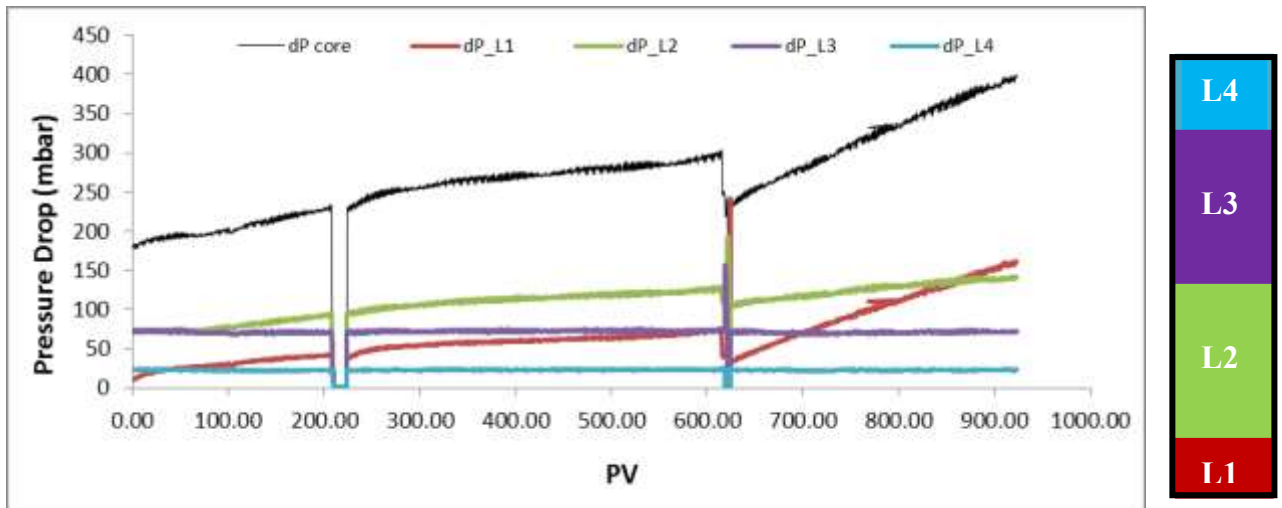


Figure 33: Pressure Drop Profile data along the core

The pressure drop profile data shows a linear pressure drop trend for the first 600 PV injected. During sampling (after injection of 600 PV) there was a change in the slope of the pressure drop trend. This change trend may be due to change of the arrangement of suspended solid particles on the injection face leads to a more compact filter cake. For the first 100 PV injected, most of the pressure drop was measured along L1 section which increase the probability of having external filter cake. After injection of 100 PV, the pressure drop starts to increase in section L2. During the whole experiment, there was no change in the pressure drop measured along both section L3 and L4 which means that most of suspended solid particles were retained in section L1 and L2. The pressure drop data was used to calculate the injectivity decline along the core as shown in figure (34). The overall injectivity decline along the core was 47.75 % from the initial injectivity. Due to the effect of the sampling on the pressure drop profile, it was decided to repeat the experiment again but without sampling this time.

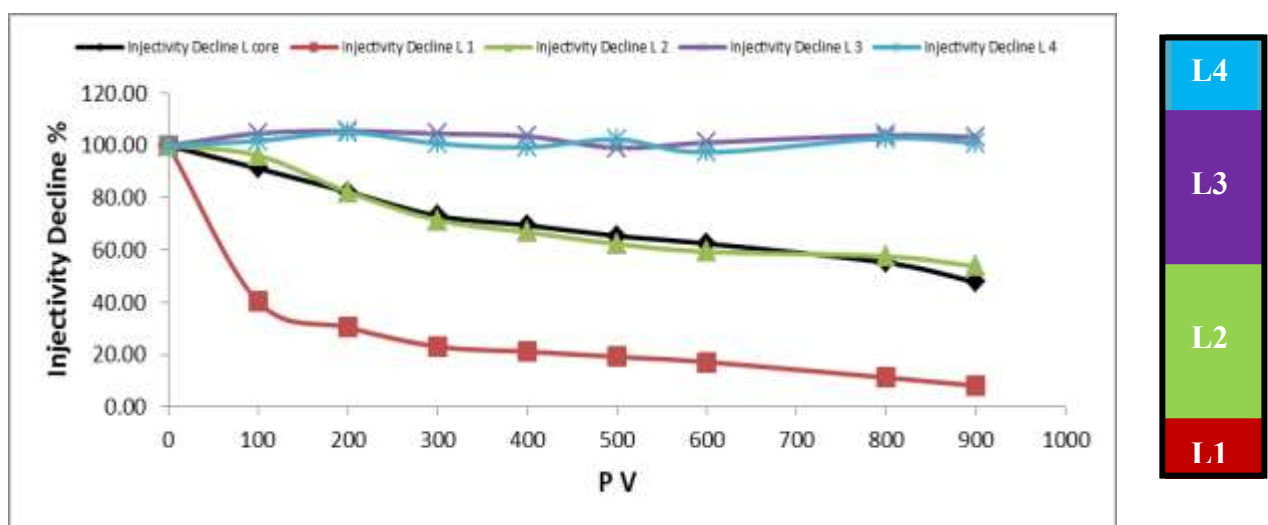


Figure 34: Injectivity Decline along the 1st core

5.5 Experiment CF-02

By applying the same procedures of the first experiment, the permeability measurements were done on the second core as mentioned in the table (5-4). Then the suspension injection was started. The flow parameters for the 2nd core flooding experiment are mentioned in table (5-5).

Segment	Permeability (Darcy) (Tap Water)	Permeability (Darcy) (Brine)	Permeability (Darcy) (After Brine Injection)
Core	2.82	2.91	2.90
Segment 01	2.33	2.47	2.22
Segment 02	2.81	2.92	2.88
Segment 03	2.83	2.90	2.93

Table (5-4): permeability measurements for 2nd core

Injection Rate	20 mL/min
Concentration	100 PPM
PH	8.1
Average Particle Size	2 μ m
Total PV Injected	1088 PV
Duration	37 hrs

Table (5-5): flow parameters for the 2nd core flooding experiment

The pressure drop profile data was similar to the first experiment figure (35). The data shows a linear pressure drop trend for the first 600 PV injected. After injection of approximately 600 PV there was a change in the slope of the pressure drop trend. This change trend may be due to change of the arrangement of suspended solid particles on the injection face leads to a more compact filter cake. For the first 100 PV injected, most of the pressure drop was measured along L1 section which increase the probability of having external filter cake. After injection of 100 PV, the pressure drop starts to increase in section L2. During the whole experiment, there was no change in the pressure drop measured along both section L3 and L4 which means that most of suspended solid particles were retained in section L1 and L2. The pressure drop data was used to calculate the injectivity decline along the core as shown in figure (36). The overall injectivity decline along the core was 34.56% from the initial injectivity

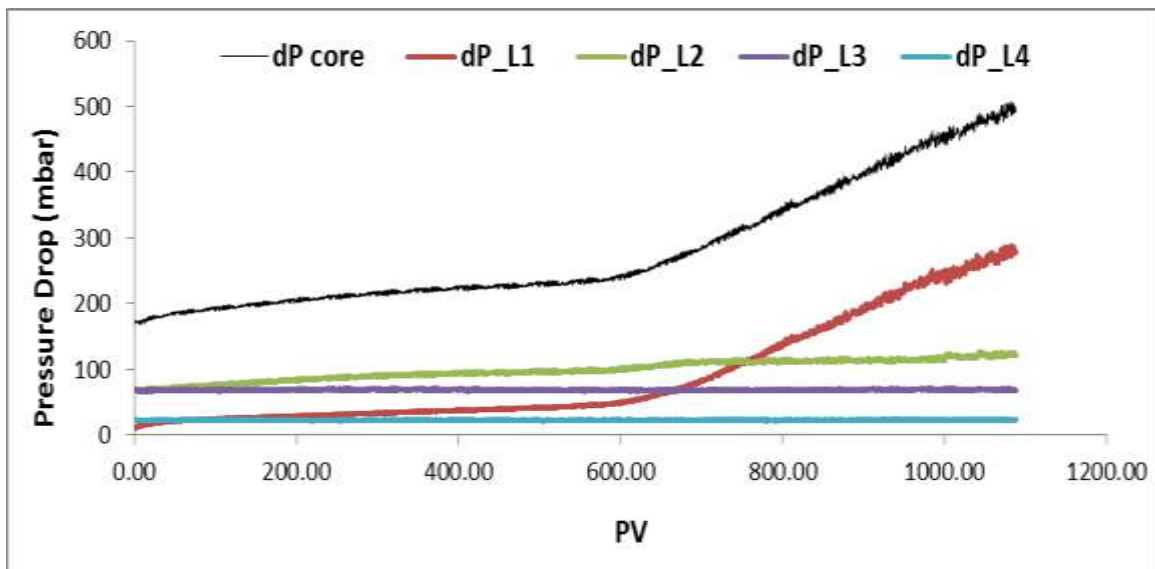


Figure 35: Pressure Drop Profile data along the 2nd core

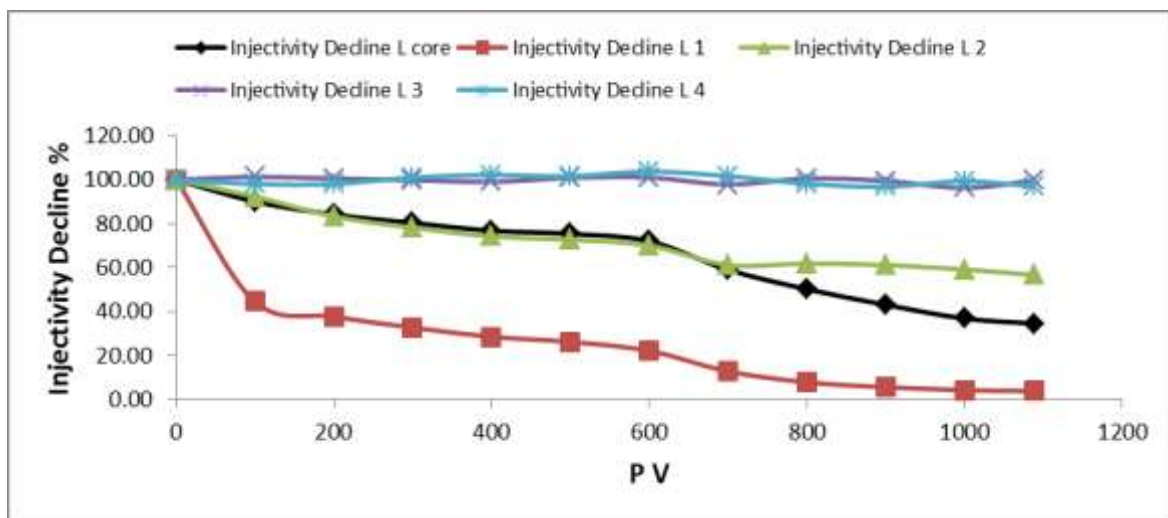


Figure 36: Injectivity Decline along the 2nd core



By the end of this experiment the permeability measurements were done. The final permeability of the core after suspension injection was 1.83 darcy. Then we apply back flow with brine without suspended particles to see if there will be enhance on permeability. The final permeability after back flow was 2.06 darcy.

Chapter Six: Conclusion and Recommendation

It was obvious from the characterization phase that the hydrodynamic particle size of Baracarb particles in different brine samples is always larger than the actual particle size. As the brine salinity increase, the average particle size increase. There is a specific PH range at which the lower value of the hydrodynamic average Baracarb particle size in the brine was observed. The concentration of Baracarb particles in brine has no clear effect on the hydrodynamic average particle size.

The pressure drop profile did not show a linear relation with the total pore volume injected. The internal core damage was limited and had a lower effect on the total pressure drop. However, the external core damage (External filter cake) had a higher effect on the pressure drop. The structure of the external filter cake changed with time and became more impermeable.

Further research work still needs to be done in this scope to validate if the suspension concentration has an effect on the pressure drop profile and as a consequence affect the injectivity. Moreover, different flow rates should be applied to understand its effect on the formation damage. Furthermore, introducing coagulating fluid such as oil in water can has also impact on injectivity decline which need to be investigated.

References

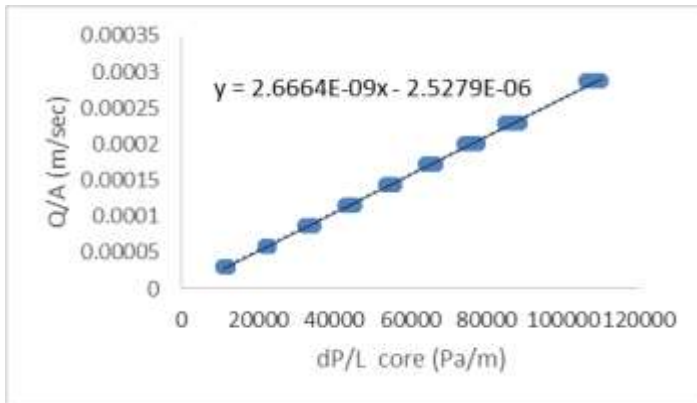
- [1] Al-Abduwani, F.A.H. 2005. Internal Filtration and External Filter Cake Build-up in Sandstones. PhD Dissertation, Delft University of Technology, Delft. ISBN 90-9020245-5.
- [2] Murtaza A. 2017. Injectivity Decline in Ultra-Filtered Water Flooding of High Permeability Sandstone Reservoirs. Master thesis, Delft University of Technology, Delft. <http://resolver.tudelft.nl/uuid:2b5bb61e-3e55-4842-b22b-d7bff68c1adf>
- [3] Farajzadeh R. 2004. Produced Water Re-Injection (PWRI) An Experimental Investigation into Internal Filtration and External Cake Build up. Master thesis, Delft University of Technology, Delft. TA/PW/04-14
- [4] Trefalt G. and Borkovec M. 2014. Overview of DLVO Theory. Short notes, Laboratory of Colloid and Surface Chemistry (LCSC), University of Geneva.
- [5] Yerramilli R. 2012. Water Injectivity Prediction: Experiments and Modeling. Master thesis, Delft University of Technology, Delft. AES/PE/12-17.
- [6] A. H. De Zwart, "Investigation of clogging processes in unconsolidated aquifers near water supply wells," 2007.
- [7] M. Elimelech, J. Gregory, and X. Jia, Particle deposition and aggregation: measurement, modelling and simulation. Butterworth-Heinemann, 2013.
- [8] P. Vilks, H. Miller, and D. Doern, "Natural colloids and suspended particles in the Whiteshell Research Area, Manitoba, Canada, and their potential effect on radiocolloid formation," Applied Geochemistry, vol. 6, no. 5, pp. 565-574, 1991.
- [9] J. N. Ryan and M. Elimelech, "Colloid mobilization and transport in groundwater," Colloids and surfaces A: Physicochemical and engineering aspects, vol. 107, pp. 1-56, 1996.
- [10] W. Stumm, Chemistry of the solid-water interface: processes at the mineral-water and particle-water interface in natural systems. John Wiley & Son Inc., 1992.
- [11] A. A. Tchistiakov, "Colloid chemistry of in-situ clay-induced formation damage," in SPE International Symposium on Formation Damage Control, 2000: Society of Petroleum Engineers.
- [12] J. Herzig, D. Leclerc, and P. L. Goff, "Flow of suspensions through porous media—application to deep filtration," Industrial & Engineering Chemistry, vol. 62, no. 5, pp. 8-35, 1970.
- [13] F. Civan, "Formation damage mechanisms and their phenomenological modeling-an overview," in European Formation Damage Conference, 2007: Society of Petroleum Engineers.
- [14] N. Lenchenkov and C. van Kruijsdijk, "Conformance Control in Heterogeneous Oil Reservoirs with Polymer Gels and Nano-Spheres."
- [15] R. Lawson, T. Gresham, I. Richardson, F. Siega, and S. Addison, "LONG RUN POLYMERIZATION EXPERIMENTS AT THE KAWERAU GEOTHERMAL LIMITED POWER PLANT," in Proceedings 38th New Zealand Geothermal Workshop, 2016, vol. 23, p. 25.
- [16] T. Coradin, D. Eglin, and J. Livage, "The silicomolybdic acid spectrophotometric method and its application to silicate/biopolymer interaction studies," Journal of Spectroscopy, vol. 18, no. 4, pp. 567-576, 2004.
- [17] A. C. Todd, J. Somerville, and G. Scott, "The application of depth of formation damage measurements in predicting water injectivity decline," in SPE Formation Damage Control Symposium, 1984: Society of Petroleum Engineers.
- [18] P. Shutong and M. M. Sharma, "A model for predicting injectivity decline in water-injection wells," SPE Formation Evaluation, vol. 12, no. 03, pp. 194-201, 1997.
- [19] P. G. Bedrikovetsky, C. J. A. Furtado, A. Siqueira, and A. L. S. de Souza, "A comprehensive model for injectivity decline prediction during PWRI," in European Formation Damage Conference, 2007: Society of Petroleum Engineers.
- [20] P. G. Bedrikovetsky, E. J. Mackay, R. M. Silva, F. M. Patricio, and F. F. Rosário, "Produced water re-injection with seawater treated by sulphate reduction plant: Injectivity decline, analytical model," Journal of Petroleum Science and Engineering, vol. 68, no. 1, pp. 19-28, 2009.
- [21] J. Veil, "US produced water volumes and management practices in 2012," Oklahoma City, OK: Ground Water Protection Council, 2015.
- [22] C. Clark, C. Harto, J. Sullivan, and M. Wang, "Water use in the development and operation of geothermal power plants," Argonne National Laboratory (ANL)2010.
- [23] J. Herzig, D. Leclerc, and P. L. Goff, "Flow of suspensions through porous media—application to deep filtration," Industrial & Engineering Chemistry, vol. 62, no. 5, pp. 8-35, 1970.
- [24] O. Vetter and V. Kandarpa, "Reinjection and injection of fluids in geothermal operations (state of the art)," Vetter Research, Costa Mesa, CA (USA)1982.

- [25] F. Civan, "Formation damage mechanisms and their phenomenological modeling-an overview," in European Formation Damage Conference, 2007: Society of Petroleum Engineers.
- [26] C. Gruesbeck and R. Collins, "Entrainment and deposition of fine particles in porous media," Society of Petroleum Engineers Journal, vol. 22, no. 06, pp. 847-856, 1982.
- [27] L. Costier, P. J. van den Hoek, C. J. Davidson, M. Ding, H. van den Berg, and R. Hofland, "Predicting Water Injection Dynamics by Leading-edge Coreflood Testing," in EUROPEC/EAGE Conference and Exhibition, 2009: Society of Petroleum Engineers.
- [28] T. Hofsaess and W. Kleinitz, "30 Years of Predicting Injectivity after Barkman & Davidson: Where are we today?," in SPE European Formation Damage Conference, 2003: Society of Petroleum Engineers.
- [29] A. Vaz Jr, P. G. Bedrikovetsky, C. J. A. Furtado, A. G. Siqueira, and A. L. S. de Souza, "Effects of Residual Oil on Re-Injection of Produced Water," in SPE Europec/EAGE Annual Conference and Exhibition, 2006: Society of Petroleum Engineers.
- [30] F. Civan, Reservoir formation damage. Gulf Professional Publishing, 2015.
- [31] A. Kalantariasl et al., "Injectivity during PWRI and Disposal in Thick Low Permeable Formations (Laboratory and Mathematical Modelling, Field Case)," in SPE European Formation Damage Conference and Exhibition, 2015: Society of Petroleum Engineers.
- [32] J. H. Barkman and D. H. Davidson, "Measuring water quality and predicting well impairment," Journal of Petroleum Technology, vol. 24, no. 07, pp. 865-873, 1972.

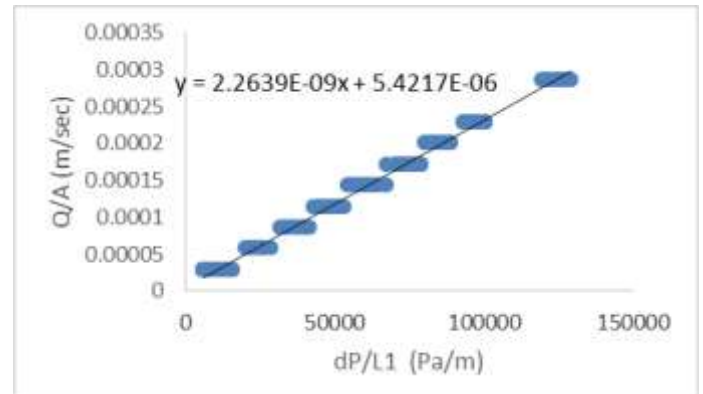
Appendix A: Permeability Measurements

A.1: CF-01 (tap water)

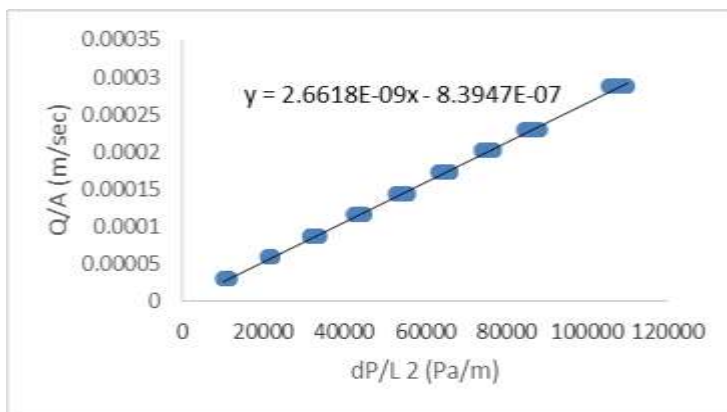
Pressure Gradient across L Core



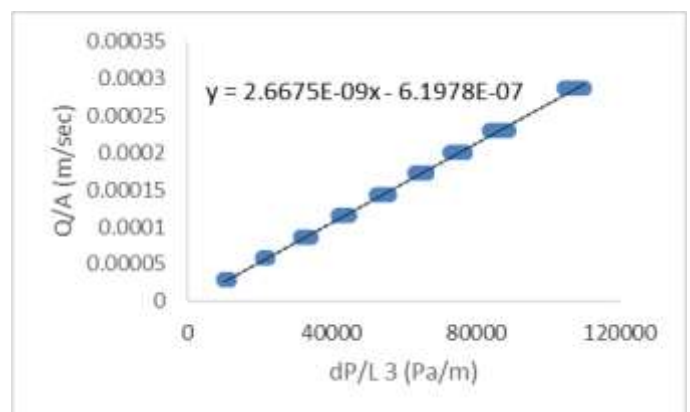
Pressure Gradient across L1



Pressure Gradient across L2

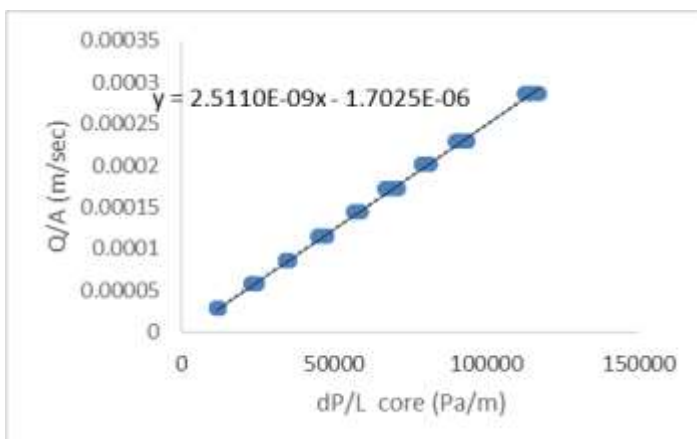


Pressure Gradient across L3

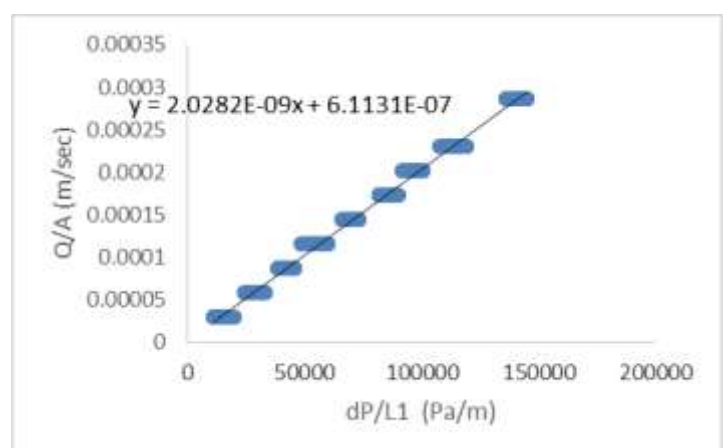


A.2: CF-01 (Brine)

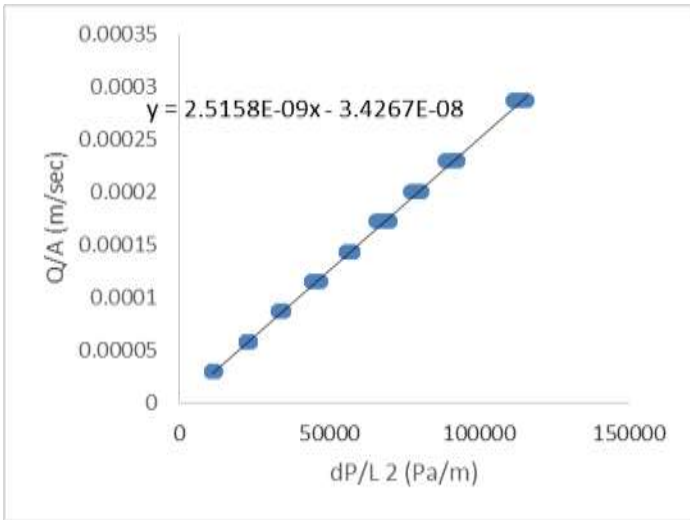
Pressure Gradient across L Core



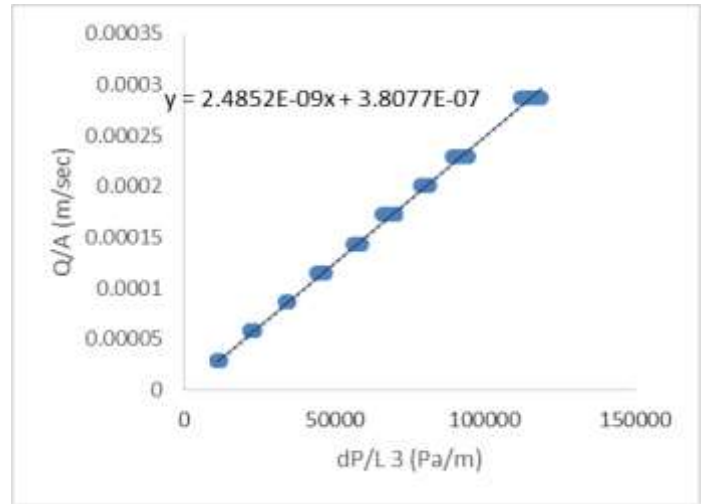
Pressure Gradient across L1



Pressure Gradient across L 2

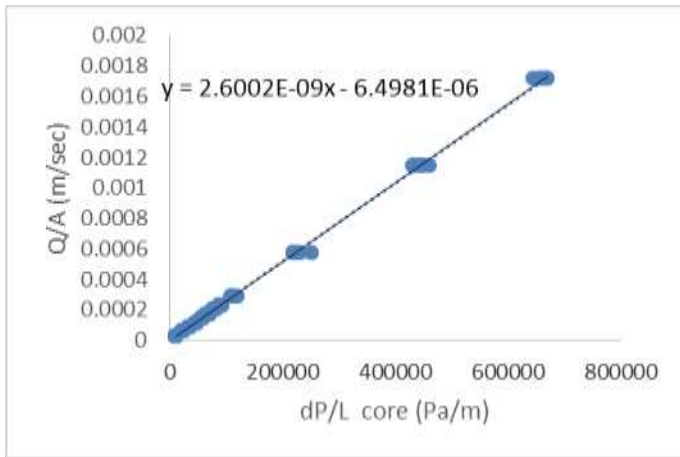


Pressure Gradient across L3

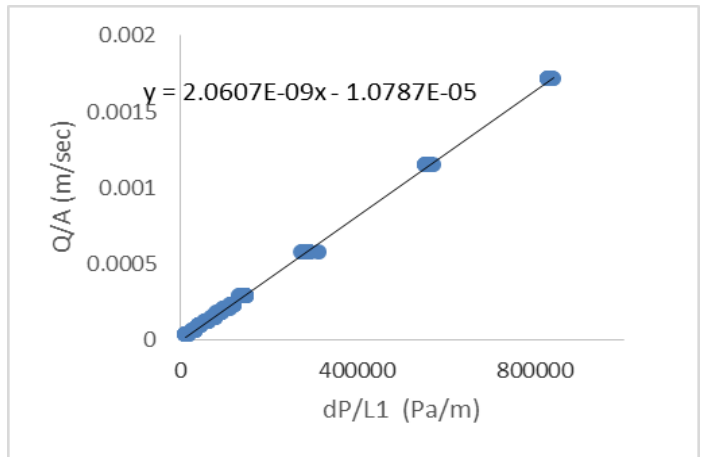


A.3: CF-01 (after the injection of 75 PV of Brine)

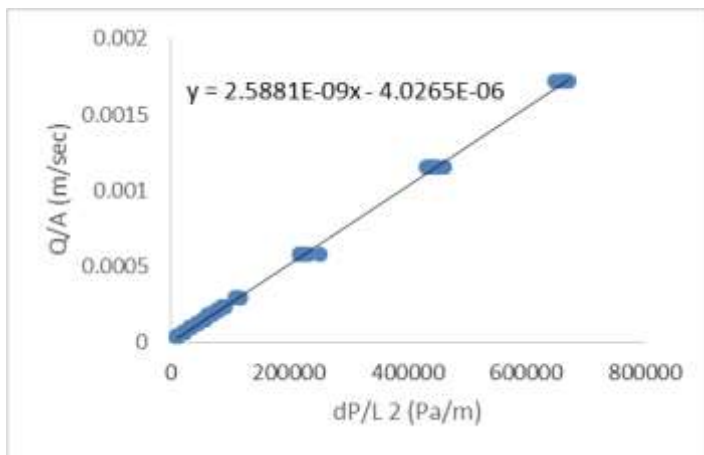
Pressure Gradient across L Core



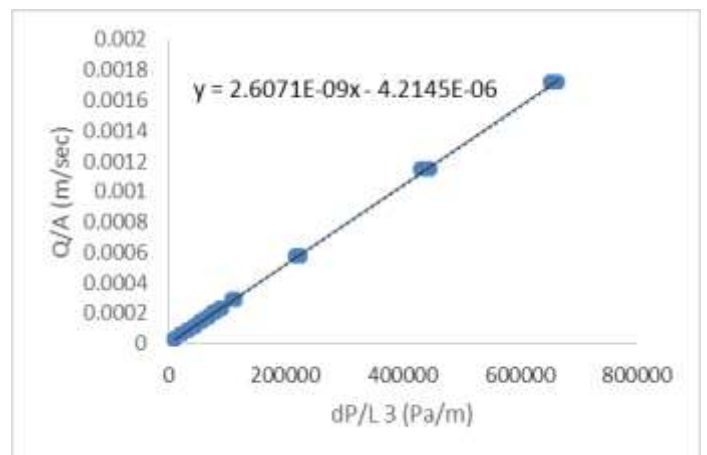
Pressure Gradient across L1



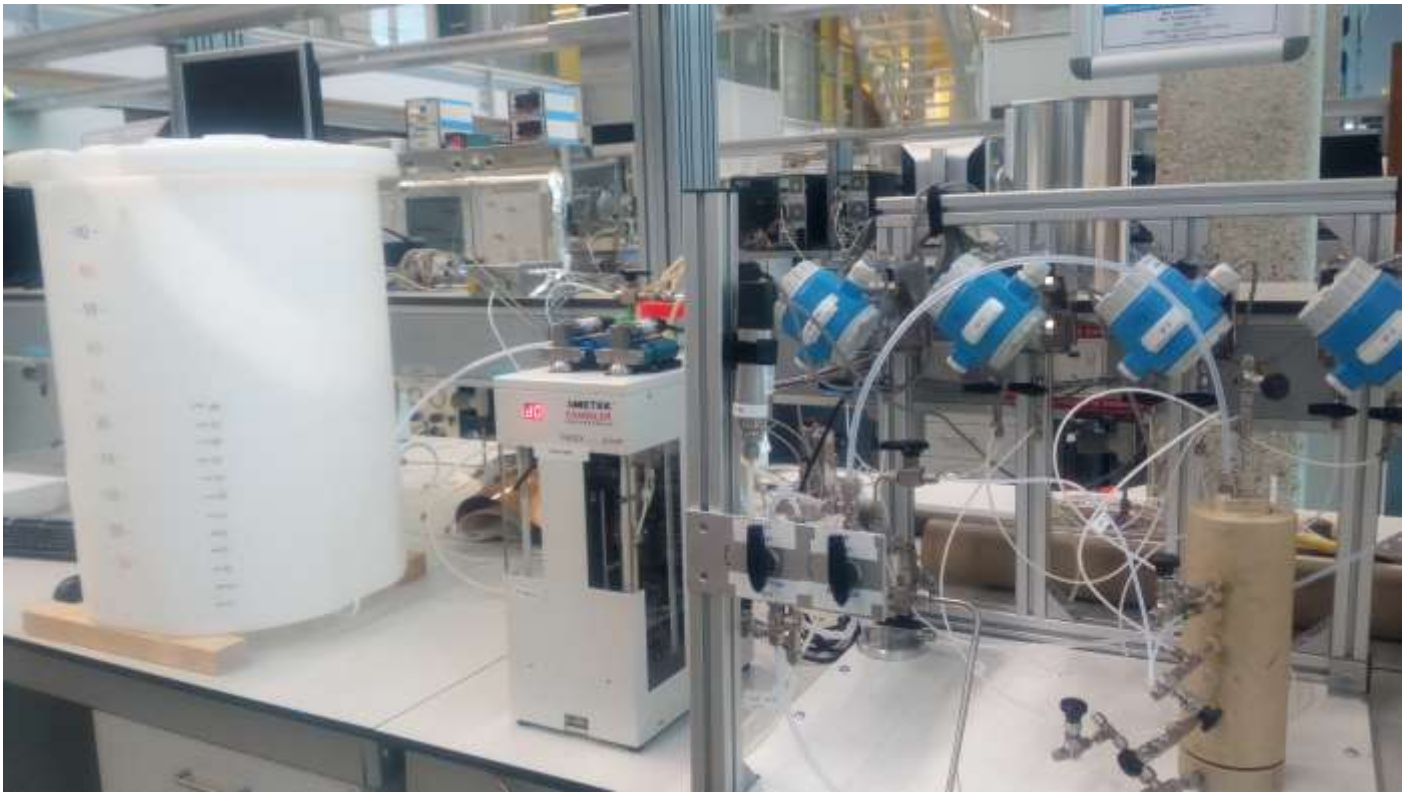
Pressure Gradient across L 2



Pressure Gradient across L3



Appendix B: Picture of the Experimental Setup



Quizix Precision Pumps



Core Holder



Mixing Tank



Differential Pressure Gauge



Absolute Pressure Gauge



Back Pressure Valve